Ann. Rev. Fluid Mech. 1986. 18:91–147
Copyright © 1986 by Annual Reviews Inc. All rights reserved

ANNUAL REVIEWS Further
Quick links to online content

Annu. Rev. Fluid Mech. 1986.18:91-147. Downloaded from www.annualreviews.org
by Marine Biological Laboratory - Woods Hole Oceanographic Institution on 04/18/13. For personal use only.

EDDIES, WAVES, CIRCULATION, AND MIXING: Statistical Geofluid Mechanics

Greg Holloway

Institute of Ocean Sciences, P.O. Box 6000, Sidney,
British Columbia, V8L 4B2, Canada

1. INTRODUCTION

1.1 *Turbulent and Not-So-Turbulent Geofluids*

The complexity of geophysical flows, from scales of planetary radius down to scales of molecular diffusion, has long posed a fascinating and frustrating challenge to fluid dynamicists. It is not only a tantalizing theoretical question but also one of practical importance. Despite determined study, understanding of the oceans and atmosphere and, especially, the prediction of responses to our trespasses upon these environments remain dangerously suspect.

Much of the dynamical difficulty arises from nonlinear coupling across many scales of motion. Occasionally one refers to the "turbulent atmosphere" or the "turbulent ocean." Just as often it is remarked that these systems are not altogether "turbulent" if that adjective is taken to connote a condition that is highly chaotic, dissipative, diffusive, or possessed of whatever other attributes that one may assign to "turbulence." Examples of wavelike phenomena abound but often are partly obscured by nonlinear interactions. Persistent, coherent, finite-amplitude flow features also are observed.

Moreover there is the disturbingly nontrivial problem of distinguishing mean and fluctuating fields. Geophysical flows often are characterized by spectra, both in frequency and in wave number, that are continuous and "red" in character. Then the definition of a mean field becomes more or less

0066–4189/86/0115–0091$02.00

arbitrary. This problem is compounded when we ask the dynamical question, how are mean and fluctuating fields interrelated?

1.2 *Approaches*

Faced with this complexity, what is to be done? On the one hand, ever bigger and faster computers will provide ever more power to numerical hydrodynamical approaches in which a wide range of scales of motion are explicitly resolved. The computer approach has its weaknesses: It raises both the inevitable question of how much does any solution depend upon numerical method and how much upon physics, and also the need to organize the output of such numerical empiricism according to some conceptual framework.

On the other hand, traditional theoretical approaches have tended to fall into two areas. Specific flow mechanisms, say a kind of wave propagation or an instability, might be isolated and solved analytically. The question then is how to obtain the collective result of many such mechanisms acting in a common environment; it is a "forest-and-trees" problem. The second theoretical approach is exemplified by turbulence theories such as those that rest upon dimensional analyses, similarity assumptions, or heuristics. Such theories yield statistical information on collective behavior. However, when the underlying mechanisms become more elaborate (e.g. including both wave propagation and turbulent advection), then the problem becomes ambiguous to dimensional analysis, may not support similarity assumptions, and can be quite confusing to heuristic approaches.

This review concerns a third kind of theoretical approach. We consider the exercise of ideas from equilibrium and disequilibrium statistical mechanics as applied to macroscale geophysical flows. The literature discussing these applications to geophysical flows is relatively recent, mostly going back less than a decade. Earlier developments are due to Onsager (1949), Hopf (1952), and Lee (1952). We provide here an overview of the methods of equilibrium and disequilibrium statistical mechanics (Sections 3 and 4). These sections are brief, conceptual, and nonspecific. The major part of this review is then the discussion in Section 5 of specific examples illustrating a wide variety of geophysical applications. The reader who finds the conceptual overview esoteric may be surprised to see the detailed quantitative calculations that result from applications. A main point to be demonstrated is that these methods offer a practicable approach to problems that otherwise perforce fall into the domains of numerical empiricism or of heuristic description. Moreover, one obtains directly the relation of statistical quantities to other statistics, which also reveals an analytical dependence upon external parameters.

It is to be emphasized that this article is organized along lines of

Annu. Rev. Fluid Mech. 1986.18:91-147. Downloaded from www.annualreviews.org
by Marine Biological Laboratory - Woods Hole Oceanographic Institution on 04/18/13. For personal use only.

methodology; no effort is made to provide a systematic treatment of the phenomenology of geofluids, for which a number of reviews and textbooks are available.

2. GEOFLUID EVOLUTION IN PROBABILITY

Consider a typical geofluids problem. The problem will often be expressed in the form of a nonlinear partial differential equation with boundary conditions, symbolically

$$\frac{\partial}{\partial t}\xi + \mathscr{L}\xi + \mathscr{N}\xi\xi = \mathscr{E}, \qquad \mathscr{B}\xi = \mathbf{0} \quad \text{on } C, \tag{1}$$

where $\mathscr{L}$, $\mathscr{N}$, and $\mathscr{B}$ are operators on a vector field ξ. Here $\mathscr{L}$ and $\mathscr{B}$ are taken to be linear, while $\mathscr{N}$ is a bilinear operator. Components of ξ might include velocity components, density, pressure, elevation, concentrations, or whatever else is of interest. The vector $\mathscr{E}$ represents external forcing. Nonlinearity in (1) is only of second degree, such as is often introduced by advection. Boundary conditions are given as homogeneous for simplicity. More general cases than (1) may be considered; here we assume only that (1) is illustrative of many problems.

We seek to represent the solution $\xi(\mathbf{x}, t)$ on a basis set as

$$\xi(\mathbf{x}, t) = \sum_{i=1}^{M} \mathbf{y}_i(t)\phi_i(x), \tag{2}$$

where the ϕ_i are chosen in some convenient, orthogonal way, perhaps as eigenfunctions of $\mathscr{L}$ satisfying $\mathscr{B}$ (although this need not be the case). An important remark is that (2) has been truncated at some large but finite M. If the dimension of each amplitude vector $\mathbf{y}_i$ is R, then the total number of degrees of freedom is RM.

The truncation in (2) raises difficult issues. An argument that is often used is that variations across short length scales, which tend to be less energetic than larger scale motions, might be ignored or else "averaged over" so as to be represented by "eddy diffusivity," for example. However, such heuristic "averaging," when performed at synoptic or mesoscales of atmospheres and oceans, has won notoriety for generating wrong results. In principle we might suppose M so large as to express scales of motion down to the scales of molecular diffusivity.

Substituting (2) into (1) and enforcing the truncation at M produces

$$\dot{\mathbf{y}}_i + \sum_{j=1}^{M} L_{ij}\mathbf{y}_j + \sum_{j}^{M}\sum_{k}^{M} N_{ijk}\mathbf{y}_j\mathbf{y}_k = e_i, \tag{3}$$

Annu. Rev. Fluid Mech. 1986.18:91-147. Downloaded from www.annualreviews.org
by Marine Biological Laboratory - Woods Hole Oceanographic Institution on 04/18/13. For personal use only.

where $\dot{\mathbf{y}}_i$ is the time rate of change of amplitude vector $\mathbf{y}_i$. We may conceptualize (3) as describing the motion of a point Y tracing a trajectory in a phase space of very large dimension RM spanned by coordinates $\{\mathbf{y}_i\}$.

There are two attitudes that we may adopt toward (3). One approach is to pick $Y(0)$ and solve for $Y(t)$. Unless expressions for L, N, and e are especially simple, a solution for $Y(t)$ requires resorting to numerical integration. However, both a practical and a theoretical difficulty arise. The practical difficulty is that for large M the computer demand can become excessive. Moreover, in the case of weather forecasting or, especially, in the case of ocean-circulation calculation, a condition for sufficiently large M is not known. The resulting $Y(t)$ may be grossly unfaithful to a "true" Y according to (1).

The theoretical difficulty is a greater problem. Even if $Y(t)$ as calculated is close to "true" Y, Equation (1) may still have the property that two solutions commencing from slightly different initial conditions, but subject to the same $\mathscr{B}$ and $\mathscr{E}$, will move off along rapidly diverging trajectories, becoming as dissimilar from each other as two randomly selected Y. Since initial conditions for real geofluids are hardly ever known precisely in all details, the different initial conditions may be practically indistinguishable, whereas the ensuing evolution produces very distinctive conditions. Similar sources of uncertainty may enter through $\mathscr{B}$ and $\mathscr{E}$. Under such circumstances any particular solution for $Y(t)$ becomes useless after some "predictability time."

Given that exact trajectories of geofluids are neither practically nor even theoretically available, it is appropriate to pose such problems differently. Consider instead a time-evolving probability density $p(Y, t)$ for finding a geofluid in the neighborhood of Y at time t. One may think of p as a number density in a large ensemble of realizations. Then "conservation of trajectories" provides the evolution equation for p:

$$\frac{\partial}{\partial t} p + \nabla_Y \cdot (p\dot{\mathbf{Y}}) = 0, \tag{4}$$

where ∇_Y is the RM-dimensional gradient operator on the phase space and $\dot{\mathbf{Y}}$ is the rate of displacement, or "phase-space velocity," of a geofluid at Y.

In some cases the equation of motion may satisfy

$$\nabla_Y \cdot \dot{\mathbf{Y}} = 0, \tag{5}$$

whence (4) becomes

$$\frac{\partial}{\partial t} p + \dot{\mathbf{Y}} \cdot \nabla_Y p = 0, \tag{6}$$

so that p "flows" as an RM-dimensional incompressible fluid in the phase space. If the representation (2) is such that the $\mathbf{y}_i$ are canonical coordinates,

Annu. Rev. Fluid Mech. 1986.18:91-147. Downloaded from www.annualreviews.org
by Marine Biological Laboratory - Woods Hole Oceanographic Institution on 04/18/13. For personal use only.

then (5) is the statement of Hamilton's equations. Assurance of this property may motivate a development in Hamiltonian dynamics; in many cases though one may prefer to test (5) directly under a representation chosen for some other convenience. Indeed for most cases, including those with forcing and dissipation, (5) and (6) will not hold. When (6) holds, the system is said to have the Liouville property.

Now we might contemplate assigning an initial $p(Y, 0)$ and then solving (4) for $p(Y, t)$, from which we could evaluate the expectation of $Y(t)$ or moments thereof. However, for any realistically complicated expression for $\mathbf{Y}$ and any RM larger than a few, direct solution for $p(Y, t)$ is usually infeasible. Moreover, beyond such practical difficulties, there is a theoretical reason why $p(Y, t)$ might not be sought.

Recollect that we introduced p in part on account of the inability to observe Y precisely. Thus $p(Y, 0)$ would be distributed over some phase volume that represents the minimum volume element within which we might discriminate different Y. Although $p(Y, 0)$ occupies such a volume, subsequent straining-shearing-stirring of p by $\dot{\mathbf{Y}}$ following (4) will produce smaller phase-space scales in p. To be consistent, we must identify such small scales in p to be unobservable with regard to, say, calculations of expectations of Y. Therefore we consider instead a probability density $\hat{p}$, which represents an averaging of p over the smallest observable phase volume.

Here we subscribe to the classical concept of "coarse graining" (cf. Tolman 1950). It can be seen that $\hat{p}$ will evolve differently from p. Consider, for example, an evolution of p satisfying the Liouville property. If p is initially highly concentrated, it must remain so while, perhaps, being drawn out into ever thinner filaments. Individual filaments become too thin to be resolved by any observing system, and hence $\hat{p}$ perforce must average p over the minimum observable phase volume. Such averaging represents an irretrievable loss of information and introduces time irreversibility into a dynamical system that otherwise might satisfy time-reversal symmetry. Geophysical fluid dynamics (GFD) researchers are reminded that planetary rotation needs also to be reversed in time-reversal arguments. Although p remains concentrated, it often appears to dilute, thereby filling a larger phase volume. The reader may be amused that this description of probability evolving in phase space is so like an initially concentrated pollutant dispersing in some geofluid system [see, for example, Haidvogel & Keffer (1984) or Holloway & Kristmannsson (1984)].

3. EQUILIBRIUM STATISTICAL MECHANICS

This section concerns the exercise of the "maximum-entropy principle," or (effectively) the Second Law of Thermodynamics, with regard to macro-

Annu. Rev. Fluid Mech. 1986.18:91-147. Downloaded from www.annualreviews.org
by Marine Biological Laboratory - Woods Hole Oceanographic Institution on 04/18/13. For personal use only.

scale geophysical flows. We are not concerned here with usual thermodynamics such as might describe an equation of state of seawater. Indeed, we can avoid some areas of confusion by proceeding more from the view of information theory (Khinchin 1957, Jaynes 1957, Katz 1967, Levine & Tribus 1979) than from conventional statistical mechanics.

The central concept is the system entropy, which we regard as a measure of the uncertainty, or "missing information," in the inability to observe or forecast Y precisely. This entropy may be distinguished from the thermodynamic specific entropy of the fluid, although it is noteworthy, following Jaynes (1957), that the dynamical account developed here may be extended to include the thermodynamic entropy. However, we do not include thermodynamic entropy except indirectly as manifested, for example, through viscous heating.

Let us recall the concept of entropy as developed by Shannon (Shannon & Weaver 1949) and Wiener (1948). Suppose a random process A may select one of n discrete states with probability P_i for the ith state. We seek a function H that measures the uncertainty of outcome of A, subject to two conditions:

1. The greatest uncertainty is when all outcomes are equally probable. Thus H is to be a maximum for $P_i = 1/n$.
2. If a second random process B is independent of A, then a measure of uncertainty of joint outcome is the sum of the separate uncertainties. That is, $H_{AB} = H_A + H_B$.

Given these conditions, Shannon showed that, uniquely within a multiplicative constant,

$$H = -\sum_i P_i \ln P_i. \tag{7}$$

Some corollaries of (7) are noteworthy. If the outcome is certain, say $P_i = \delta_{ik}$, then H takes a minimum value of zero. (We evaluate $P_i \ln P_i = 0$ when $P_i = 0$.) If processes A and B are partially dependent, then H_{AB} behaves reasonably, including the case when B is an identical copy of A (for which $H_{AB} = H_A$).

For processes yielding continuously distributed outcomes, e.g. the coordinate values of Y in phase space, (7) becomes

$$H = -\int dY\, \hat{p}(Y) \ln \hat{p}(Y), \tag{8}$$

where the integration is over all phase space. It could be assumed that an undetermined measure $m(Y)$ multiplies the integrand in (8); however, Salmon (1982b,c) argues that preservation of the Liouville property, apart

Annu. Rev. Fluid Mech. 1986.18:91-147. Downloaded from www.annualreviews.org
by Marine Biological Laboratory - Woods Hole Oceanographic Institution on 04/18/13. For personal use only.

from forcing and dissipation, requires that m be independent of Y. Also to be noted in (8), we consider the observable (in principle) $\hat{p}$ rather than p; thus H is the experimental entropy (Jaynes 1957).

Given an isolated system in which forcing and dissipation are excluded, the Second Law reads

$$\frac{d}{dt} H \geq 0, \tag{9}$$

where we consider continuous evolution in time and it is understood that (9) holds as an ensemble average. It is remarkable that the Second Law enters axiomatically, defining an "arrow of time," unanticipated by the other laws of dynamics. The central concept of equilibrium statistical mechanics follows directly: $\hat{p}(Y, t)$ is expected to approach a condition giving a maximum value of H.

Evaluation of $\hat{p}$ that maximizes H is performed under certain constraints. One constraint is the normalization condition

$$\int dY\, \hat{p} = 1. \tag{10}$$

For most systems, some representation of total energy $E(Y)$ will be conserved. Thus $E(Y) = E_0$ as given by initial conditions, and we might constrain p to satisfy

$$\langle E \rangle \equiv \int dY\, \hat{p} E = E_0. \tag{11}$$

Other invariants, such as total mass or angular momentum, may provide further constraints. Of particular GFD importance is the conservation of potential vorticity following fluid elements. Defining potential enstrophy $Q(Y)$ as the square of potential vorticity integrated over the flow domain, we often have the constraint that $Q(Y) = Q_0$.

The manner in which constraints such as E_0 and Q_0 are imposed admits some possible choices. If we strictly require $E(Y) = E_0$ and $Q(Y) = Q_0$, then the $\hat{p}$ yielding maximum entropy is

$$\hat{p}(Y) = C\, \delta(E(Y) - E_0)\, \delta(Q(Y) - Q_0), \tag{12}$$

the "microcanonical ensemble." However, calculations of moments of Y (for example, the energy spectrum) can be difficult. Equilibrium spectra for two-dimensional turbulence have been calculated from (12) by Basdevant & Sadourny (1975), revealing the complexity of such calculations.

An alternative to (12) that proves easier to manipulate is the "macrocanonical ensemble." For positive-definite invariants such as E or Q,

Annu. Rev. Fluid Mech. 1986.18:91-147. Downloaded from www.annualreviews.org
by Marine Biological Laboratory - Woods Hole Oceanographic Institution on 04/18/13. For personal use only.

exercise of the method of Lagrange multipliers to maximize H subject to (10), (11), and a like condition on Q yields

$$\hat{p}(Y) = C \exp [-\alpha_1 E(Y) - \alpha_2 Q(Y)], \tag{13}$$

where C is a normalization, and α_1 and α_2 are Lagrange multipliers.

Under (13) we note that each trajectory is not required to lie on the surface $E = E_0$, $Q = Q_0$. This may be a point of consternation, since (dynamically) each trajectory preserves E and Q. The algebraic forms of (12) and (13) appear to be quite different, and so a choice of one or the other should have significant consequences. However, for most of the questions one might ask regarding most GFD systems, differences between (12) and (13) prove insignificant following a calculation given by Khinchin (1957) and extended by Salmon et al. (1976; hereafter SHH). Usually we are concerned only with marginal probability, often for a single mode as, say, $\hat{p}_i(y_i)$. Asymptotic methods for integration over (12) then yield

$$\hat{p}_i(y_i) = C_i \exp (-\alpha_1 E_i - \alpha_2 Q_i), \tag{14}$$

where E_i and Q_i are single-mode contributions to E and Q. Validity of (14) requires that E_i and Q_i be small compared with E and Q for all i. Since (14) would result also from (13), differences between (12) and (13) are not important as regards $\hat{p}_i$. If we are interested in calculating expectations such as $\langle E_i \rangle$ or $\langle Q_i \rangle$, then we are only concerned with (14).

The interesting results to be obtained from equilibrium statistical mechanics methods depend upon specific expressions for $E(Y)$, $Q(Y)$, or other constraints. There are surprises, such as cases when predictable, steady, large-scale flow rises from chaotic initial conditions while expressing the tendency to increase entropy. These and other cases are described in Section 5.

For now we recognize two deficiencies of equilibrium statistical mechanics. Firstly, while a state of maximum H can be described, no information is given concerning the rapidity with which a system approaches maximum H. Secondly, and more fundamentally, the atmosphere and oceans and the life systems that inhabit these environments are not isolated, closed systems. Rather, these systems receive and release energy, exchanging information with a larger universe. In particular, earth-atmosphere-ocean life systems receive high-temperature (low-entropy) solar radiation while collectively reradiating low-temperature (high-entropy) earth radiation. It is thus natural to seek a statistical geofluid mechanics that makes explicit the generation of entropy. For a quantitative treatment of systems that are maintained far from maximum H through the roles of forcing and dissipation, we turn to the less well-developed field of disequilibrium statistical mechanics.

Annu. Rev. Fluid Mech. 1986.18:91-147. Downloaded from www.annualreviews.org
by Marine Biological Laboratory - Woods Hole Oceanographic Institution on 04/18/13. For personal use only.

4. DISEQUILIBRIUM STATISTICAL MECHANICS

Among various methods that might come under the heading "disequilibrium statistical mechanics," only moment-hierarchy closure methods have found significant geophysical application to date. We limit our discussion here to such moment closures. The relation of these moment closures to entropy generation is explicit and consistent with the Second Law; cf. (9). However, alternatives are certainly possible—for example, methods based upon the direct approach toward solving the Liouville equation (4) (cf. the exploration by Thompson 1983).

To retain a tractable problem, we limit our interest to describing the evolution of second-order correlations $\langle y_i y_j \rangle$. Calculations prove practicable in the homogeneous environment for which $\langle y_i y_j \rangle$ is diagonal in (i,j). The limitation to homogeneity is severe. However, statistics $\langle y_i y_i \rangle$ contain much geophysically relevant information, including energy spectra, tracer transports, and buoyancy flux.

The connection between second-order correlations and entropy has been developed by Carnevale et al. (1981). Defining H_2 as the maximum of H from (8) under prescribed $\langle y_i y_j \rangle$, they found that

$$H_2 = \ln \det \langle y_i y_j \rangle, \tag{15a}$$

or, if $\langle y_i y_j \rangle$ is diagonal in (i,j),

$$H_2 = \sum_i \ln \det \langle y_i y_i \rangle. \tag{15b}$$

In (15b), the determinant is of the component matrix $\langle yy \rangle$ in mode i. For many applications, this may be the total energy E_i in mode i. Then

$$H_2 = \sum_i \ln \langle E_i \rangle, \tag{15c}$$

a form that has been used by Montgomery (1976).

We seek to develop equations for the evolution of correlations $\langle \mathbf{yy} \rangle$. Previous developments in the hydrodynamic context have addressed separately problems of weakly nonlinear wave-wave interaction (Hasselmann 1962, 1967, Benney & Saffman 1966, Benney & Newell 1969) or fully developed turbulence [Kraichnan 1959, Edwards 1964, Herring 1965, and works reviewed by Leslie (1973) and Orszag (1977)]. For many GFD problems a separation between waves and turbulence is untenable and, moreover, may prove unnecessarily frustrating. At the level of a conceptual overview, it is easy to adopt a unified approach to waves and turbulence. Some detailed results are made more apparent in Section 5.

There are various methods for developing moment hierarchy closures.

Annu. Rev. Fluid Mech. 1986.18:91-147. Downloaded from www.annualreviews.org
by Marine Biological Laboratory - Woods Hole Oceanographic Institution on 04/18/13. For personal use only.

Here we sketch one of the simpler schemes, referred to as the "eddy-damped quasi-normal Markovian" (EDQNM) method, which may be viewed as an abridgment of more formal systems such as the "direct-interaction approximation" (Kraichnan 1959). In abbreviated notation, recall Equation (3):

$$\frac{\partial}{\partial t} y + Ly + Nyy = e. \tag{16}$$

Let us here take $\langle y \rangle = 0$, hence omitting mean-motion fields. In some of the illustrations to follow, this limitation may be lifted or, in other cases, relaxed somewhat. We also return to this point in Section 6.

From (16), it follows that

$$\frac{\partial}{\partial t} \langle yy \rangle + L\langle yy \rangle + N\langle yyy \rangle = \langle ey \rangle, \tag{17}$$

where L and N are considered to be deterministic and e is stochastic. Even if we suppose that $\langle ey \rangle$ is given, (17) is not suitable for calculation, since $\langle yyy \rangle$ is not determined.

Continuing from (16), we have

$$\frac{\partial}{\partial t} \langle yyy \rangle + L\langle yyy \rangle + N\langle yyyy \rangle = \langle eyy \rangle. \tag{18}$$

Throughout this review, arguments of **y** are considered to be simultaneous; that is, we treat only single time statistics. Apart from $\langle eyy \rangle$, a solution for $\langle yyy \rangle$ is still not possible on account of $\langle yyyy \rangle$. Continuing to write equations for successively higher moments only leads to an unclosed hierarchy—hence the "closure problem."

Closure is usually effected by considering fourth-order correlations, which (for $\langle y \rangle = 0$) can be expressed as

$$\langle yyyy \rangle = \langle yy \rangle \langle yy \rangle + \langle yyyy \rangle'. \tag{19}$$

If the different modes of motion were statistically independent in their evolution, then the residual or fourth cumulant $\langle yyyy \rangle'$ would vanish.

One means of closure is called fourth-cumulant discard, which involves setting $\langle yyyy \rangle' = 0$ in (19). Weak-wave interaction theory can be achieved as a synthesis of fourth-cumulant discard together with a two-time-scale expansion such that, if L describes purely free wave propagation and $e = 0$, then for $t \to \infty$,

$$\langle yyy \rangle = -L^{-1} N \langle yy \rangle \langle yy \rangle. \tag{20}$$

Annu. Rev. Fluid Mech. 1986.18:91-147. Downloaded from www.annualreviews.org
by Marine Biological Laboratory - Woods Hole Oceanographic Institution on 04/18/13. For personal use only.

In (20), L^{-1} has singularities on a resonance manifold where the natural frequencies of the three modes sum identically to zero. For large t, L^{-1} is dominated by such singularities and can be approximated by

$$L^{-1} \approx \pi\delta(\omega_1+\omega_2+\omega_3), \tag{21}$$

where ω_1, ω_2, and ω_3 are the three natural frequencies.

Turbulence theory has followed other routes, since if L is given only by viscous dissipation, discard of $\langle yyyy\rangle'$ in (19) is known to lead to unrealizable solutions of (17) and (18) [yielding, for example, predictions of negative energy spectra (Ogura 1963)]. One approach is to attempt to replace $N\langle yyyy\rangle'$ by a term $\mu\langle yyy\rangle$, where μ is a third-order matrix of undetermined coefficients. If the coefficients in μ are positive, the effect is to induce relaxation of $\langle yyy\rangle$ toward zero. An assumption of quasi-stationarity in time is made such that a nearly steady solution to (18),

$$\langle yyy\rangle = -(L+\mu)^{-1}N\langle yy\rangle\langle yy\rangle, \tag{22}$$

is achieved on a time scale shorter than the slow evolution of $\langle yy\rangle$ according to (17). In (22) we have also ignored $\langle eyy\rangle$, as is customary but perhaps not always justified. Substituting (22) into (17) yields the desired evolution equation for $\langle yy\rangle$:

$$\frac{\partial}{\partial t}\langle yy\rangle + L\langle yy\rangle - N(L+\mu)^{-1}N\langle yy\rangle\langle yy\rangle = \langle ey\rangle. \tag{23}$$

Differences among EDQNM treatments arise from different methods of determining μ, which is assumed to depend upon the $\langle yy\rangle$. Some of these differences are described in Section 5.

Two noteworthy features of (23) are the following: First, if nonlinear interaction is strongly dominant relative to, say, wave propagation, then μ [which is presumed to increase with increasing energy $E(Y)$] will dominate $L+\mu$. Thus we will have $(L+\mu)^{-1} \approx \mu^{-1}$, which is the form that occurs in EDQNM turbulence theories. At the other limit, when nonlinearity is very weak relative to wave propagation, L dominates and L^{-1} is approximated by the resonant interaction condition (21). Thus (23) provides a smooth bridge from waves to turbulence (cf. Holloway 1979).

The second important feature of (23) is a property proven by Montgomery (1976) and Carnevale et al. (1981). The effect of the term $-N(L+\mu)^{-1}N\langle yy\rangle\langle yy\rangle$ is to yield $dH_2/dt \geq 0$, where H_2 is from (15), with $dH_2/dt = 0$ only at equilibrium as in (13). Dissipation and forcing, which can be represented in L and e, may either increase or decrease H_2; they represent external couplings in open systems.

Annu. Rev. Fluid Mech. 1986.18:91-147. Downloaded from www.annualreviews.org
by Marine Biological Laboratory - Woods Hole Oceanographic Institution on 04/18/13. For personal use only.

5. ILLUSTRATIONS

Whereas the foregoing discussions have been broad and conceptual, the remainder of this paper consists of a gallery of specific illustrations. The intent is to explore a diversity of GFD applications and to demonstrate the quantitative as well as qualitative utility of the resulting calculations.

A number of the following geophysical applications derive from an equation of motion appropriate to quasi-geostrophic, multiple-layer flow that we here record as

$$\frac{\partial}{\partial t} q_i + J(\Psi_i, q_i) + \mathscr{D}_i(\Psi_i) = \mathscr{E}_i, \tag{24}$$

where q_i is the potential vorticity in layer i; Ψ_i is the stream-function representation of the nondivergent, quasi-horizontal velocity field in layer i; J is the Jacobian determinant with respect to horizontal coordinates; $\mathscr{D}_i$ is a dissipation operator acting on Ψ_i; and $\mathscr{E}_i$ is any external torque, such as wind-stress curl, acting upon the uppermost layer in an ocean model. The potential vorticity q_i includes relative vorticity

$$\xi_i = \hat{\mathbf{z}} \cdot \nabla \times \mathbf{u}_i = \nabla^2 \Psi_i, \tag{25}$$

as well as planetary vorticity and any potential stretching terms due to layer-thickness fluctuations or bottom topography. Specific definitions of q_i are given where needed.

5.1 *Two-Dimensional Turbulence on a Plane and on a Sphere*

This example has been thoroughly reviewed previously, especially by Kraichnan & Montgomery (1980) with interesting comments also by Rhines (1979), Salmon (1982b), and McWilliams (1983). Since many of the illustrations that follow may be seen as embellishments upon this simplest case, we recall briefly the principal results from the equilibrium and disequilibrium statistical mechanics of two-dimensional turbulence.

In planar geometry with either closed or periodic boundaries, invariants of the unforced, nondissipative motion include kinetic energy $E = \frac{1}{2}\overline{|\nabla\Psi|^2}$ and enstrophy $Z = \overline{\zeta^2}$ as well as any $V = \overline{v(\zeta)}$, where v may be any function. (Overbars denote integration over the flow demain.) The role of a possible V is sometimes a concern. However, the nature of a possible V, other than Z, appears not to restrict observable probabilities $p(Y)$. Furthermore, spectral truncation destroys the invariance of most V. An interesting remark also is made by Thompson (1982), who shows that, subject to certain restrictions, conservation of only a few invariants may determine

Annu. Rev. Fluid Mech. 1986.18:91-147. Downloaded from www.annualreviews.org
by Marine Biological Laboratory - Woods Hole Oceanographic Institution on 04/18/13. For personal use only.

the equation of motion, so that further invariants provide only redundant constraints.

Maximum-entropy solutions for $\hat{p}$ subject to specification of E and Z yield either (12) or (13), the difference being immaterial, since either tends to lead to (14) (cf. SHH). If we assume periodic conditions in coordinates $\mathbf{x}$, a natural expansion in (2) is

$$\Psi(\mathbf{x}, t) = \sum_{\mathbf{k}} \Psi_{\mathbf{k}}(t)\, e^{i\mathbf{k}\cdot\mathbf{x}}, \tag{26}$$

where $\Psi_{\mathbf{k}}$ is the expansion coefficient at wave vector $\mathbf{k}$. Ensemble-averaged modal energy and enstrophy are

$$E_{\mathbf{k}} = \tfrac{1}{2}k^2\langle\Psi_{\mathbf{k}}\Psi_{-\mathbf{k}}\rangle, \tag{27a}$$

$$Z_{\mathbf{k}} = \langle\zeta_{\mathbf{k}}\zeta_{-\mathbf{k}}\rangle = k^4\langle\Psi_{\mathbf{k}}\Psi_{-\mathbf{k}}\rangle. \tag{27b}$$

The *equilibrium* marginal probability (14) at $\mathbf{k}$ is

$$\hat{p}_{\mathbf{k}}(\Psi_{\mathbf{k}}) = \left(\frac{\alpha_1 + \alpha_2 k^2}{\pi}\right)^{1/2} \exp\left(-(\alpha_1 + \alpha_2 k^2)\Psi_{\mathbf{k}}\Psi_{-\mathbf{k}}\right), \tag{28}$$

from which

$$E_{\mathbf{k}} = \frac{1}{2}\frac{1}{\alpha_1 + \alpha_2 k^2}, \qquad Z_{\mathbf{k}} = \frac{k^2}{\alpha_1 + \alpha_2 k^2}, \tag{29}$$

as obtained by Kraichnan (1967) and verified repeatedly in numerical experiments by Fox & Orszag (1973), Carnevale (1982), and Bennett & Haidvogel (1983), among others. Moreover, Carnevale (1982) has calculated the evolution of entropy (15c), showing its rise to the anticipated experimental equilibrium value. The evolution of the energy spectrum and of the entropy is shown in Figure 1.

The equilibrium distribution has been calculated in spherical geometry by Frederiksen & Sawford (1980). Expansion (2) becomes

$$\Psi(\lambda, \mu, t) = \sum_m \sum_n \Psi_{mn}(t) P_n^m(\mu)\, e^{im\lambda}, \tag{30}$$

where λ is longitude, μ is latitude, and P_n^m are associated Legendre functions. The sums on m and n may be truncated according to various schemes.

If a variable χ_{mn} is defined as

$$\chi_{mn} = \tfrac{1}{2}[(2-\delta_{m0})n(n+1)]^{1/2}\Psi_{mn}, \tag{31}$$

then the modal energy and enstrophy are

$$E_{mn} = \langle|\chi_{mn}|^2\rangle, \qquad Z_{mn} = n(n+1)E_{mn}. \tag{32}$$

In addition to the above invariants, motion on the sphere also conserves

Annu. Rev. Fluid Mech. 1986.18:91-147. Downloaded from www.annualreviews.org
by Marine Biological Laboratory - Woods Hole Oceanographic Institution on 04/18/13. For personal use only.

Ψ_{01} and $|\Psi_{11}|$ in the absence of any surface friction or topographic roughness. This is a consequence of angular-momentum conservation but does not affect the equilibrium distributions for E_{mn} and Z_{mn}. Corresponding to (29), we have

$$E_{mn} = \frac{1/2}{\alpha_1 + \alpha_2 n(n+1)}. \tag{33}$$

Here it is interesting that the mean rotation of the fluid does not affect the equilibrium spectrum (33). A similar outcome is seen in the following illustration regarding β-plane motion, where it is found that the value of β does not affect the *equilibrium* statistics.

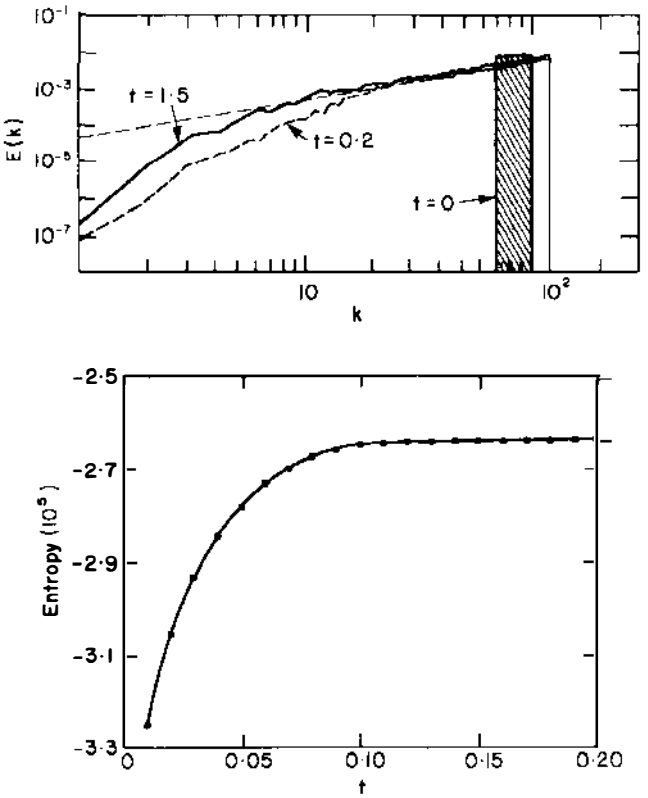

Figure 1 Evolution of inviscid two-dimensional turbulence toward absolute equilibrium is seen from direct numerical simulation. (*Top*) Kinetic-energy spectra are shown for the initial conditions and at two later times. The equilibrium spectrum is shown dashed. (*Bottom*) Entropy rises quickly to the equilibrium value for an isolated realization (Carnevale 1982).

Annu. Rev. Fluid Mech. 1986.18:91-147. Downloaded from www.annualreviews.org
by Marine Biological Laboratory - Woods Hole Oceanographic Institution on 04/18/13. For personal use only.

Annu. Rev. Fluid Mech. 1986.18:91-147. Downloaded from www.annualreviews.org
by Marine Biological Laboratory - Woods Hole Oceanographic Institution on 04/18/13. For personal use only.

Disequilibrium treatment of two-dimensional turbulence has been explored mainly for the case of planar geometry. Early, more-or-less heuristic accounts by Kraichnan (1967) and Batchelor (1969) reveal the dominant phenomenology. Kraichnan's account especially emphasizes the dual-cascade scenario in which excitation forced in a wave-number band near, say, k_0 decomposes to a uniform spectral flux of enstrophy toward higher wave number together with a uniform spectral flux of energy toward lower wave numbers, with the latter process referred to as a "reverse cascade." In the asymptotic limit of very wide ranges of available wave number, energy transfer tends to vanish on the enstrophy-flux subrange, while enstrophy transfer tends to vanish on the energy-flux subrange. Dimensional arguments anticipate power-law behavior as $k^{-5/3}$ on the energy-flux subrange $k < k_0$ and as k^{-3} on the enstrophy-flux subrange $k > k_0$. Corrections for wave-number nonlocal effects may be applied to the k^{-3} subrange.

Some support for these accounts was soon obtained from numerical experiments by Lilly (1971, 1972) and others. The extent of similarity to observed transfer processes in the Earth's atmosphere is discussed by Boer & Shepherd (1983).

Detailed closure-theoretical accounts such as (23) were developed by Leith (1971), Orszag (1970, 1977), Kraichnan (1971a,b), and others. Evolution of the closure studies, including careful testing against numerical experiments, has been examined by Herring et al. (1974) and Poquet et al. (1975), with a thorough review given by Kraichnan & Montgomery (1980). Closure-theoretical treatment on the sphere is more algebraically tedious and has been pursued only to a limited extent (e.g. Legras 1980), with numerical experiments having been performed by Tang & Orszag (1978) and Basdevant et al. (1981). Here only the briefest mentions have been made as a prelude to the extensions from these studies that are reviewed in the following sections.

5.2 *Beta-Plane Turbulence*

Rhines (1975, 1977, 1979) obtained insight into this problem for the case of β-plane flow, periodic in x (east) and y (north), for which the equation of motion in one layer is (24) with $q = \zeta + \beta y$. This problem interests us here for two reasons: (*a*) There are striking differences between the equilibrium and disequilibrium statistical mechanics, and (*b*) the problem is a simple prototype for waves/turbulence interaction.

Under periodic boundary conditions, without forcing or dissipation, integral invariants are $\overline{|\nabla\Psi|^2}$ and $\overline{\zeta^2}$, where overbars denote integration over the periodic domain. Invariants are just as in the case of two-dimensional turbulence. It is also the case that $\overline{q^2}$ is conserved, but this

proves redundant insofar as $\overline{\zeta y}$ may be set to zero by statistical homogeneity. Thus for $\mathscr{D} = 0 = \mathscr{E}$ and finite spectral truncation, the flow field approaches (29), which is independent of the value of β. In particular, (29) is isotropic. This would *appear* to contradict numerical experiments by Rhines (1975), Williams (1978), and others that reveal a marked propensity for the flow field to evolve toward anisotropy-favoring zonal velocity components over meridional components. Such anisotropy is also evident in the larger scales of atmospheric observations (Boer & Shepherd 1983).

A seeming discrepancy with regard to anisotropic tendencies is resolved by showing that β enters only in the *disequilibrium* phenomena. A closure-theoretical treatment by Holloway & Hendershott (1977; hereafter HH) explores this waves/turbulence problem. The evolution equation corresponding to (23) is

$$\left(\frac{\partial}{\partial t} + 2\nu_k\right) Z_{\mathbf{k}} = \sum_{\substack{\mathbf{p},\mathbf{q} \\ \mathbf{k}+\mathbf{p}+\mathbf{q}=0}}^{\Delta} \theta_{\mathbf{kpq}} [a_{kpq} Z_{\mathbf{p}} Z_{\mathbf{q}} - 2 b_{kpq} Z_{\mathbf{p}} Z_{\mathbf{k}}], \tag{34}$$

where $Z_{\mathbf{k}} = \langle \zeta_{\mathbf{k}} \zeta_{-\mathbf{k}} \rangle$, $\zeta_{\mathbf{k}}$ is the Fourier coefficient of ζ at wavevector $\mathbf{k}$, and ν_k is a function of $|\mathbf{k}|$ resulting from $\mathscr{D}$. Symbol $\sum^{\Delta}$ in (34) and hereafter indicates a sum over $\mathbf{p}$ and $\mathbf{q}$ such that $\mathbf{k}+\mathbf{p}+\mathbf{q} = 0$.

Expression $(L+\mu)^{-1}$ in (23) becomes

$$\theta_{\mathbf{kpq}} = \frac{\mu_{\mathbf{k}} + \mu_{\mathbf{p}} + \mu_{\mathbf{q}}}{(\mu_{\mathbf{k}} + \mu_{\mathbf{p}} + \mu_{\mathbf{q}})^2 + (\omega_{\mathbf{k}} + \omega_{\mathbf{p}} + \omega_{\mathbf{q}})^2}, \tag{35}$$

where $\omega_{\mathbf{k}}$ is given by the Rossby-wave dispersion relation

$$\omega_{\mathbf{k}} = -\beta k_x / |\mathbf{k}|^2. \tag{36}$$

Coefficients a_{kpq} and b_{kpq} are algebraic factors resulting from contractions of type NN in (23). Finally, the particular treatment by HH has

$$\mu_{\mathbf{k}} = \nu_k + g^2 \sum^{\Delta} \theta_{\mathbf{kpq}} \hat{b}_{kpq} Z_{\mathbf{p}}, \tag{37}$$

where g is an undetermined empirical factor, and $\hat{b}_{kpq}$ is another algebraic coefficient following Kraichnan (1971a).

A controversial point arises in this particular treatment by HH that also concerns finite-amplitude wave-wave interactions in general. In (35), HH used the free-wave frequency (36). This is called the "bare" frequency in the terminology of renormalization methods. Whereas nonlinear interaction is represented in (35) by μ (essentially a frequency broadening), it might also be assumed that a mean frequency ω be systematically shifted from the free-wave relation (36). This problem is discussed by Kadomtsev (1965) and

Annu. Rev. Fluid Mech. 1986.18:91-147. Downloaded from www.annualreviews.org
by Marine Biological Laboratory - Woods Hole Oceanographic Institution on 04/18/13. For personal use only.

Annu. Rev. Fluid Mech. 1986.18:91-147. Downloaded from www.annualreviews.org
by Marine Biological Laboratory - Woods Hole Oceanographic Institution on 04/18/13. For personal use only.

Holloway (1979), with prescriptions for obtaining a renormalized, or "dressed," frequency given by Legras (1980) and Carnevale & Martin (1982). The calculations by Legras (1980), carried out in spherical geometry, showed that the shift of the "dressed" frequency away from the "bare" frequency is not too great for planetary waves and that results from HH ought not be significantly disturbed. However, very recent results from direct numerical simulations indicate some unexpected surprises. Both in planar geometry (D. Ramsden, unpublished) and on the sphere (J. Tribbia, unpublished), the simulations show large systematic frequency shifts in the sense of rapid westward phase propagation, especially among the shorter waves. For reasons that are not understood, the nonlinearly induced frequency shift is nearly proportional to k_x in planar geometry. Consequently, the restriction to $\mathbf{k}+\mathbf{p}+\mathbf{q}=0$ means that the frequency shift nearly identically drops out of (35). It would appear that HH were approximately correct for reasons that were not at all suspected!

It is noteworthy that wave propagation or β enters (34) only through (35), affecting the efficiency of variance transfer. Absolute equilibrium (29) yields an identical zero on the right-hand side of (34) and is thus indifferent to β. It is also for expressions such as the right-hand side of (34) that Carnevale et al. (1981) have proven $dH_2/dt > 0$. However, the *rate* of increase of entropy will be depressed by wave propagation.

For what values of β is wave propagation significant compared with nonlinear interaction? An estimate can be based upon (35) by asking when terms in ω become significant. As a rough cut we may ignore the nearness to frequency resonance, i.e. to $\omega_{\mathbf{k}}+\omega_{\mathbf{p}}+\omega_{\mathbf{q}}=0$, and just compare representative ω with representative μ. For a flow with an rms velocity u' and an rms vorticity ζ', a representative length scale is $l=u'/\zeta'$, for which a representative ω is $\beta u'/\zeta'$. HH show that at scales near l, one obtains roughly $\mu=\zeta'$. Hence the relative importance of β is given as a nondimensional number

$$\hat{\beta}=\beta u'/\zeta'^2. \tag{38a}$$

A condition $\hat{\beta}=O(1)$ may be seen as a threshold for "overturning" of potential vorticity contours when $q=\zeta+\beta y$.

Rhines (1975) described the evolution of the energy spectrum as an "arrest" of the two-dimensional turbulent reverse-energy cascade toward low wave number (Kraichnan 1967) near a wave number $k_\beta=(\beta/2u')^{1/2}$. A heuristic basis for this k_β was obtained by comparing representative wave phase speed with u'. The argument leading to (38a) implies that ω be compared with ζ', suggesting that a transitional wave number be defined as

$$\hat{k}_\beta=\beta/\zeta'. \tag{38b}$$

Then the cascade arrest is seen theoretically to result from small values of $\theta_{\mathbf{kpq}}$ over $|\mathbf{k}| < \hat{k}_\beta$, suppressing transfer into these scales. In practice there is little distinction between k_β and $\hat{k}_\beta$, which become equivalent when $\hat{\beta} = O(1)$.

More striking is the evolution of anisotropy on the β-plane. Moderate k_x and small k_y are associated with large ω, whereas moderate k_y and small k_x are not. Thus the reverse cascading energy continues to transfer into $|\mathbf{k}| < \hat{k}_\beta$ for modes with small or zero k_x—hence the zonal flows. Evaluation of (34) confirms the evolution toward anisotropy at small $|\mathbf{k}|$ but also predicts persistent anisotropy favoring zonal motion at all higher $|\mathbf{k}|$ as well. The latter result would not be anticipated from simpler waves/turbulence heuristics after Rhines (1975). Numerical experiments confirm the closure-theoretical prediction for anisotropy across the spectrum, as seen in Figure 2.

5.3 *Geostrophic Turbulence Above Topography*

This problem is one of special fascination, since it is characterized by the emergence of organized, predictable, large-scale flow from random initial conditions. Classically, such organized motions might be associated with dissipation (Prigogine 1980) or, in some instances, with evolution into solitons (Rizzoli 1982, 1984). In the present problem, such organized flow arises solely as a direct manifestation of nondissipative absolute equilibrium.

In the simplest case, we consider one-layer flow on an f-plane in which the depth of fluid $H(x, y)$ varies in some complicated way suggestive of terrestrial topography. If we write

$$H(x, y) = H_0(1 - f^{-1}h(x, y)),$$

then (for $h^2 \ll f^2$) the equation of motion is (24) with $q = \zeta + h$. Without forcing or dissipation, the invariants are kinetic energy and total enstrophy, i.e.

$$\tfrac{1}{2}\overline{|\nabla\Psi|^2} \quad \text{and} \quad \overline{(\zeta + h)^2}, \tag{39}$$

leading to absolute equilibrium statistics

$$\langle \zeta_{\mathbf{k}} \zeta \qquad \frac{k^2}{\alpha_1 \quad \alpha_2} \qquad \frac{\alpha_2^2 k^4 \langle h_{\mathbf{k}} h_{-\mathbf{k}} \rangle}{\alpha_1 \quad \alpha_2} \tag{40a}$$

$$\langle \zeta_{\mathbf{k}} h_{-\mathbf{k}} \rangle = -\frac{\alpha_2 k^2 \langle h_{\mathbf{k}} h_{-\mathbf{k}} \rangle}{\alpha_1 + \alpha_2 k^2}, \tag{40b}$$

where $h_{\mathbf{k}}$ are Fourier coefficients of h, and α_1 and α_2 are determined in order to satisfy invariants (39). Corresponding solutions for barotropic flow on a

Annu. Rev. Fluid Mech. 1986.18:91-147. Downloaded from www.annualreviews.org
by Marine Biological Laboratory - Woods Hole Oceanographic Institution on 04/18/13. For personal use only.

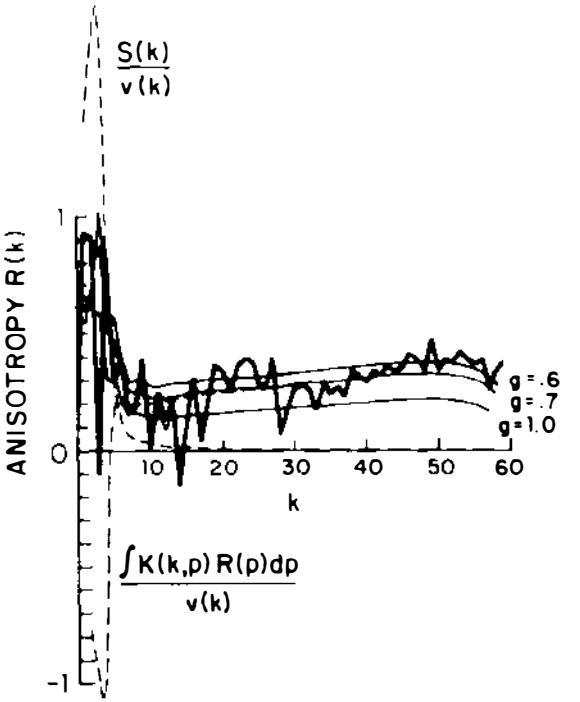

Figure 2 Disequilibrium anisotropy of β-plane turbulence is shown from numerical simulation (heavy trace) and from closure theory (light traces). The anisotropy measure $R(k)$ denotes a predominance of zonal over meridional velocities at any scale k^{-1}. The light traces show dependence upon a "test-field model" parameter (Kraichnan 1971a), which had previously been estimated by Herring et al. (1974) to take a value near $g = 0.65$. Closure theory here permits analysis of mechanisms controlling anisotropy. A dashed curve shows a source term $S(k)$, which gives the direct induction of anisotropy due to β, divided by a return-to-anisotropy coefficient ν. Nonlinear transfer of anisotropy is governed by a kernel $K(k, p)$ and is seen to account for persistent anisotropy at large wave number. Negative transfer under $K(k, p)$ is also seen to be an effective restraint upon anisotropy induced by β at small k (Holloway & Hendershott 1977).

sphere including topography have been noted by Frederiksen & Sawford (1981), Frederiksen (1982), and Sawford & Frederiksen (1983). It is noteworthy that we may permit here nonvanishing first moments. We then consider a specific realization of h, taking ensemble averages over ζ for given h. Resulting first moments [cf. (40b)] are

$$\langle \zeta_{\mathbf{k}} \rangle = -\frac{\alpha_2 k^2 h_{\mathbf{k}}}{\alpha_1 + \alpha_2 k^2} \tag{41}$$

Annu. Rev. Fluid Mech. 1986.18:91-147. Downloaded from www.annualreviews.org
by Marine Biological Laboratory - Woods Hole Oceanographic Institution on 04/18/13. For personal use only.

or, in configuration space,

$$\left(\frac{\alpha_1}{\alpha_2} - \nabla^2\right)\langle\Psi\rangle = h. \tag{42}$$

For most geophysical values of (39), it is the case that $\alpha_1/\alpha_2 < 0$, so that (42) is a forced Helmholtz equation.

This may seem surprising: that from randomly chosen initial ζ characterized by $\langle\zeta\rangle = 0$ there arises a steady, deterministic, macroscale flow given by (41) or (42). In addition to the steady component, there will occur a time-dependent part whose variance is given by the first term on the right-hand side of (40a).

The spontaneous emergence of such large-scale, organized flow has been noted for some time in numerical simulations (Holloway & Hendershott 1974, Bretherton & Haidvogel 1976) and is seen in Figure 3. In most cases, such numerical simulations have included dissipative effects and, sometimes, external forcing. Indeed, Bretherton & Haidvogel attribute the organized, steady flow to the following argument (here abbreviated):

If dissipation acts selectively on the highest wave numbers, then it is argued that total enstrophy decays more quickly than does energy. A solution is obtained that minimizes enstrophy subject to constant energy and given h. This solution describes a steady flow having many features qualitatively similar to (42), which become identical to (42) if one considers just the case where enstrophy in (39) is given its minimum value.

A controversy has ensued between advocates of the minimum-enstrophy principle and proponents of the maximum-entropy principle. Physical arguments for minimizing enstrophy may be intuitive and have been further advanced by Rhines (1979) and Leith (1984), whereas the maximization of entropy seems foreign to many researchers in GFD. However, in the absence of any dissipation and hence with no decay of enstrophy, evolution toward maximum entropy including the steady component (42) is readily seen in numerical experiments.

To go beyond extremal principles into the forced/dissipative or statistically time-evolving cases requires the treatment using disequilibrium methods. This has been done by Herring (1977) and by Holloway (1978), with the latter author obtaining a pair of equations for the coupled evolution of $\langle\zeta_{\mathbf{k}}\zeta$ ζ

$$\left(\frac{d}{dt} + 2\nu_k\right)\langle\zeta_{\mathbf{k}}\zeta_{-\mathbf{k}}$$ ζ ζ (43a)

$$\left(\frac{d}{dt} + \nu_k\right)\langle\zeta_{\mathbf{k}}h_{-\mathbf{k}}\rangle = -\eta_{\mathbf{k}}\langle\zeta$$ (43b)

Annu. Rev. Fluid Mech. 1986.18:91-147. Downloaded from www.annualreviews.org
by Marine Biological Laboratory - Woods Hole Oceanographic Institution on 04/18/13. For personal use only.

Annu. Rev. Fluid Mech. 1986.18:91-147. Downloaded from www.annualreviews.org
by Marine Biological Laboratory - Woods Hole Oceanographic Institution on 04/18/13. For personal use only.

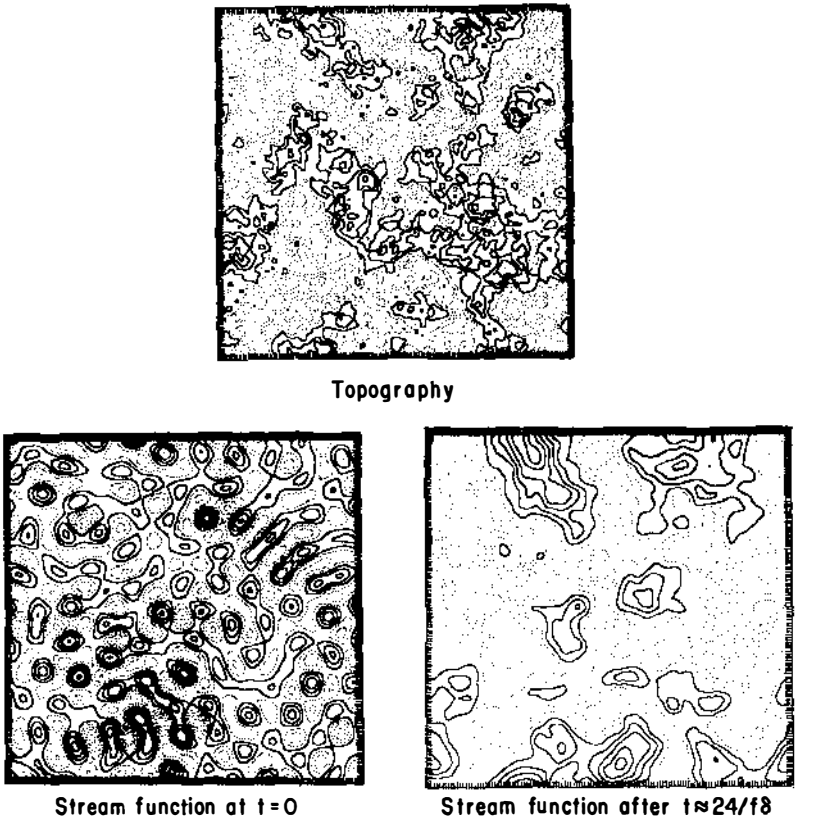

Figure 3 An initially random eddy field, shown as a stream function at $t = 0$, is permitted to decay freely in the presence of realistically complex topographic relief. After a time of approximately $24/f\delta$, where f is the Coriolis parameter and δ is characteristic relief as a fraction of total depth of fluid, it may be seen that the stream function bears a striking visual resemblance to underlying topography (Holloway & Hendershott 1974).

where $\nu_{\mathbf{k}}$ expresses dissipation and $F_{\mathbf{k}}$, $\eta_{\mathbf{k}}$, and $\sigma_{\mathbf{k}}$ are expressions involving weighted sums over spectra of ζ and h and may also include any external forcing.

Some important points concerning (43) should be noted. Firstly, these are the equations for which Carnevale et al. (1981) showed that $dH_2/dt \geq 0$, which leads to (40) in the absence of forcing and dissipation. Secondly, evolution according to (43) has been tested and found to give very good quantitative agreement in comparison with direct numerical simulation, as seen in Figure 4.

Annu. Rev. Fluid Mech. 1986.18:91-147. Downloaded from www.annualreviews.org
by Marine Biological Laboratory - Woods Hole Oceanographic Institution on 04/18/13. For personal use only.

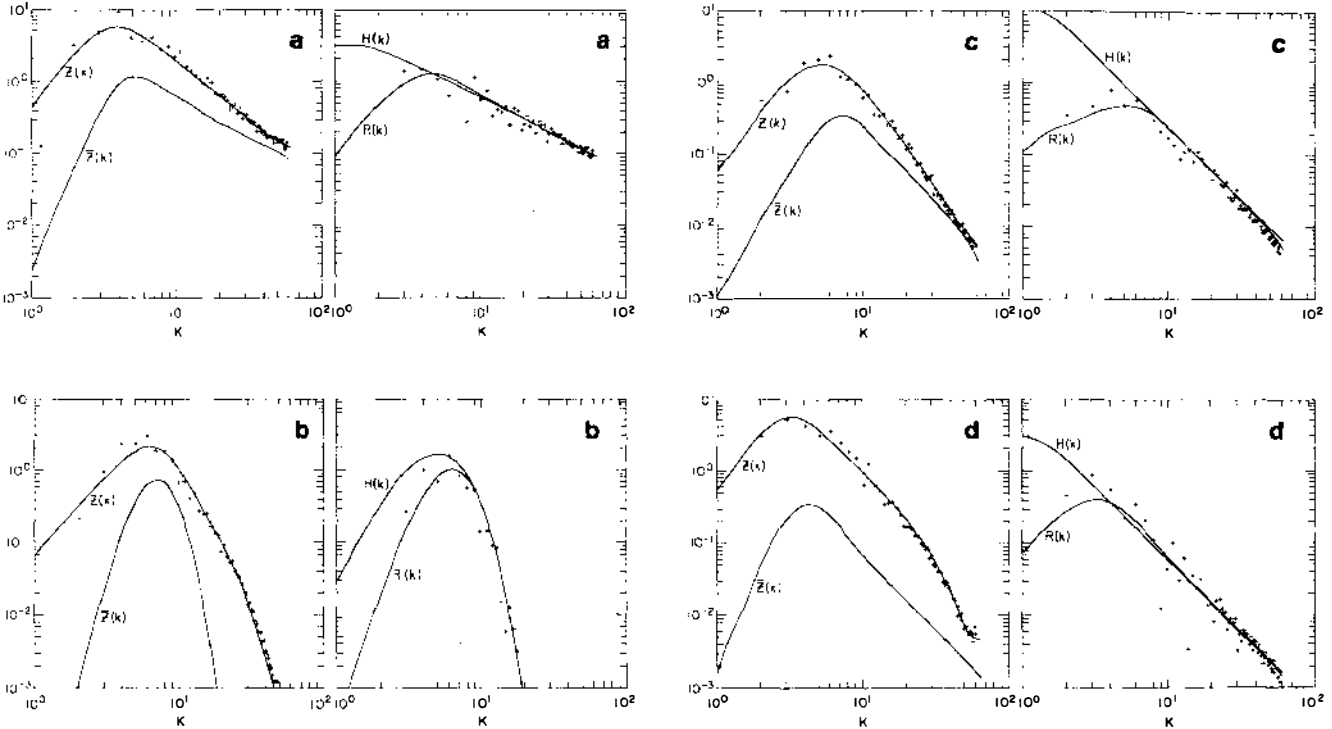

Figure 4 Closure theory is tested against numerical simulations of geostrophic eddies above complicated topography for a variety of choices of topographic interactions and different strengths of eddy fields. Spectra of topography are marked $H(k)$. Theory predicts spectra of total vorticity variance $Z(k)$ and of variance $\bar{Z}(k)$ for the steady part of the vorticity field. Also predicted is the vorticity-topography correlation, here marked $R(k)$. Crosses mark values of $Z(k)$ and $R(k)$ collected from simulation experiments. (*a*) Topography has a broad, shallow spectrum; (*b*) topography has a narrow-band spectrum; (*c*) topography is given a steep "red" spectrum. (*d*) topography has the same spectral shape as in (*c*) but is reduced in amplitude, so that the ratio of vorticity to topography is about four times greater than in (*c*) (Holloway 1978).

Annu. Rev. Fluid Mech. 1986.18:91-147. Downloaded from www.annualreviews.org
by Marine Biological Laboratory - Woods Hole Oceanographic Institution on 04/18/13. For personal use only.

5.4 *Closed-Basin Circulation and Western Intensification*

A synthesis of the preceding illustrations is seen when we consider one-layer flow in a closed, flat-bottomed, β-plane basin. Consider a case with no external forcing, no internal dissipation, and free-slip sidewall conditions. Integral invariants are kinetic energy, total enstrophy, and circulation, i.e.

$$\tfrac{1}{2}\overline{|\nabla\Psi|^2},\ \overline{(\zeta+\beta y)^2},\ \overline{\zeta}, \tag{44}$$

where the overbars indicate integration over the basin.

The maximum-entropy solution is characterized both by a large-scale steady flow and a spectrum of time-dependent eddies. The spectrum of transient eddies is given as before by (29), while the steady component, after (42), is represented by

$$\left(\frac{\alpha_1}{\alpha_2}-\nabla^2\right)\langle\Psi\rangle=\beta(y-\alpha_3), \tag{45}$$

where α_1, α_2, and α_3 are chosen so as to satisfy (44).

That (45) is an exact solution to the inviscid, nonlinear equation of motion had been observed by Fofonoff (1954). However, there was no reason to believe that oceans should "prefer" (45). Now we see that (45) is in fact selected by the maximum-entropy principle. This may seem remarkable: that deterministic, large-scale, steady flows arise spontaneously from random initial conditions as a manifestation of *equilibrium statistical mechanics.*

Taking a value for α_3 somewhere between the maximum and minimum values of y within the basin, (45) will be characterized by broad westerly flow in the interior, with return easterly flow in boundary currents of approximate width $|\alpha_1/\alpha_2|^{1/2}$ at the northern and southern boundaries of the basin. A tendency toward westward interior flow was noted by Bretherton & Karweit (1975) in numerical experiments including rough topography on a β-plane. Bretherton & Haidvogel (1976) argue that the minimum-enstrophy principle may indicate flows qualitatively like (45). Similarly, Rhines (1979) proposes that the enstrophy cascade leading to enstrophy dissipation at small scales may cause the establishment of such basin-scale flows. Here we observe that the large-scale mean flows arise with *no* topographic roughness *nor* with any dissipation.

The *disequilibrium statistical mechanics* of closed-basin flows have not been worked out. However, a qualitative evolution can be described. Note that in a basin whose geometry is east-west symmetric, equilibrium statistics for $\langle\zeta_{\mathbf{k}}\zeta_{-\mathbf{k}}\rangle$ and $\langle\Psi\rangle$ [from (29) and (45)] are also east-west symmetric. On the other hand, one of the more prominent features of real

oceans is a tendency for currents to be more intense near western basin boundaries than near eastern boundaries. Various explanations for this phenomenon have been proposed over decades of theoretical oceanographic research. Here, we propose yet another explanation.

Imagine an initial-value problem in which vorticity is randomly distributed in an ocean basin, so that $\overline{\zeta} = 0$. The initial state is characterized by $\frac{1}{2}\overline{|\nabla\Psi|^2}$ and $\overline{\zeta^2}$, from which α_1, α_2, and α_3 are determined. Without forcing or dissipation, we anticipate evolution toward (29) and (45). However, for typical geophysical values of $\frac{1}{2}\overline{|\nabla\Psi|^2}$ and $\overline{\zeta^2}$, values of α_1, α_2, and α_3 will be such that (29) will have larger $\overline{\zeta^2}$ with correspondingly smaller $\overline{\zeta y}$ (hence $\overline{\zeta y} < 0$) than are given initially. *Disequilibrium* processes must cause the changes in $\overline{\zeta^2}$ and $\overline{\zeta y}$ in order to satisfy $dH/dt > 0$. The rate of change of $\overline{\zeta^2}$ is given by

$$\frac{d}{dt}\overline{\zeta^2} = \beta \int_{y_1}^{y_2} dy |\nabla\Psi|^2 \Big|_E^W, \tag{46}$$

where the integral runs over the meridional extent of the basin, and the integrand is the difference of $|\nabla\Psi|^2$ evaluated at western and eastern boundaries. Adjustment toward maximum-entropy requires that (46) be positive and thus that $|\nabla\Psi|^2$ be larger at western boundaries. The western intensification follows in the most natural way as a Second Law manifestation (Holloway 1975). When absolute equilibrium is finally approached, western intensification must relax.

Recently this scenario has been tested by M. Smith (unpublished) using an energy/enstrophy-conserving finite-difference simulation of barotropic, quasi-geostrophic, inviscid flow in a square, β-plane basin. In addition to observing the emergence of (45), Smith noted the development and subsequent relaxation of western intensification, as shown in Figure 5.

5.5 *The Shape of the Thermocline*

Whereas we have considered barotropic motion in a closed β-plane basin of limited latitudinal extent such that βy is small compared with f_0, Salmon (1982a) has extended this treatment to a two-layer system on the equatorial β-plane. The goal is to anticipate the equilibrium form of $\langle h \rangle$, where $h(\mathbf{x}, t)$ is the thickness of the upper layer. Only the *equilibrium* statistical mechanics problem is examined.

Although equations of motion are set out in primitive form, it is convenient to calculate entropy on the assumption of nearness to geostrophy, with the equatorial singularity removed by requiring that fields remain sufficiently smooth. If the lower layer is considered to remain at rest, then the state of the system is defined approximately by $h(\mathbf{x}, t)$. Without

Annu. Rev. Fluid Mech. 1986.18:91-147. Downloaded from www.annualreviews.org
by Marine Biological Laboratory - Woods Hole Oceanographic Institution on 04/18/13. For personal use only.

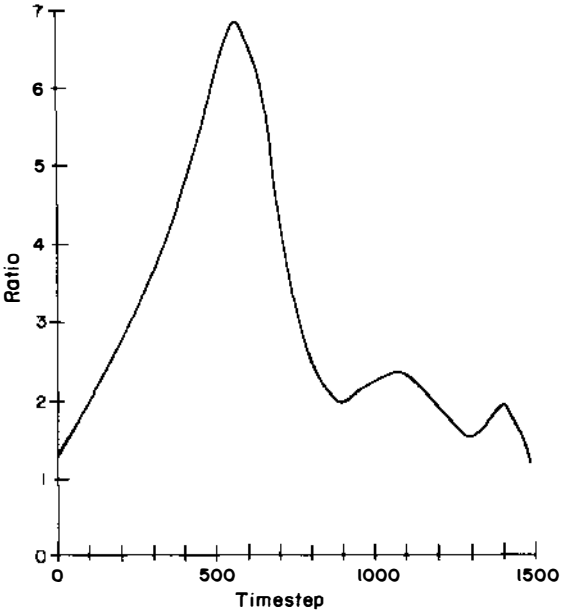

Figure 5 Time evolution of the ratio of velocity variance along the western basin margin to velocity variance along the eastern basin margin is shown from a numerical simulation of inviscid flow in a square, flat-bottomed, β-plane ocean. Western intensification occurs as a disequilibrium phenomenon associated with entropy generation and relaxes in the approach to maximum-entropy circulation (M. Smith, unpublished).

Annu. Rev. Fluid Mech. 1986.18:91-147. Downloaded from www.annualreviews.org
by Marine Biological Laboratory - Woods Hole Oceanographic Institution on 04/18/13. For personal use only.

forcing, dissipation, or property exchange between layers, the system possesses four integral constraints:

$$\text{Upper layer mass} \qquad M = \int dx\, dy\, h, \tag{47a}$$

$$\text{Energy} \qquad E = \int dx\, dy\, h \left\{ \left(\frac{g'}{\beta y} \right)^2 |\nabla h|^2 + g' h \right\}, \tag{47b}$$

$$\text{Potential vorticity} \qquad P = \int dx\, dy \left(\nabla \cdot \frac{g'}{\beta y} \nabla h + \beta y \right), \tag{47c}$$

$$\text{Enstrophy} \qquad Q = \int dx\, dy \left(\nabla \cdot \frac{g'}{\beta y} \nabla h + \beta y \right)^2 h^{-1}. \tag{47d}$$

Rather than expanding upon a basis set as in (2), Salmon (1982a) discretizes by assuming a grid-point representation on which differentials in (47) become difference operators. The upper layer is treated as a freely

evolving "blob" that covers some subset of the available grid points. The number of grid points covered or, effectively, the location of isopycnal outcrops (i.e. "blob" edge) is to be determined. For a number N_γ of points covered in configuration γ, the entropy is determined by the set of thicknesses $\{h_i\}$ at the grid points:

$$H = \sum_i^{N_\gamma} \ln \langle h_i \rangle. \tag{48}$$

However, maximization of (48) subject to (47) is difficult. A recourse is to assume approximate constraints in which each h_i is replaced by $\langle h_i \rangle$ each time it appears in the discrete representations of (47).

By considering configurations that are symmetric about the equator, it follows that $P = 0$ and thus (47c) may be omitted. Intuition may be gained by applying the remaining constraints (47) successively. Thus, if only mass (47a) is constrained, the maximum-entropy thermocline is simply flat ($h = h_0$) and covers the entire domain. Next, in addition to mass, the constraint (47d) on enstrophy is applied in a simplifying approximation

$$\sum_i \frac{\beta^2 y_i^2}{\langle h_i \rangle} = Q_0, \tag{49}$$

which leads to

$$1 = a\langle h_i \rangle + b\beta^2 y_i^2 / \langle h_i \rangle, \tag{50}$$

where a and b are constants determined from mass M_0 and enstrophy Q_0.

It may be seen that (50) is an equipartition form that recovers the previous case of mass constraint only when $b = 0$. To preserve positivity of h_i at all i, one has $a > 0, b < 0$. Then Equation (50) already has a satisfying shape: It is relatively shallow and flat near the equator and deepens with increasing latitude to either side of the equator. However, the solution suffers in that the greatest depths are attained at the highest latitudes y permitted by each N_γ. This defect is ameliorated when the energy constraint (47b) is taken into account.

Inclusion of energy conservation proves tedious. Salmon (1982a) obtains a nonlinear, fourth-order equation for $\langle h \rangle$. If a solution is attempted as a power series in y, the quartic truncation yields

$$\langle h_i \rangle = A_0 + A_2 y_i^2 + \left[-\frac{\beta^2}{8g'} + \frac{2c}{b} A_0^2 A_2 \right] y_i^4, \tag{51}$$

where $c \neq 0$ enters on account of the energy constraint. Constants A_0 and A_2 depend upon boundary conditions at "outcropping latitude" $y = y_{\max}$,

Annu. Rev. Fluid Mech. 1986.18:91-147. Downloaded from www.annualreviews.org
by Marine Biological Laboratory - Woods Hole Oceanographic Institution on 04/18/13. For personal use only.

which the fluid is free to establish. However, if these boundary conditions are

$$h = 0 \quad \text{and} \quad \frac{d}{dy}\left(\frac{g'}{\beta y}\frac{dh}{dy}\right) + \beta y = 0$$

at $y = \pm y_{max}$, then it is required that $c = 0$. To retain $c \neq 0$, a term y^6 must also be retained in (51).

It may be surprising that the double-lobed thermocline shape (thin and shallow across the equator and then achieving maximum depth at higher latitudes before turning upward at yet higher latitudes) follows from equilibrium statistical mechanics alone. To illustrate the process of adjustment, Salmon (1982a) also integrated a Lagrangian finite-element numerical model in which an initially quiescent lens of upper-layer fluid was released over the equator. Although the numerical model included friction, spontaneous evolution *toward* the higher-entropy thermocline shape was noted.

5.6 *Baroclinic Turbulence; Eddy Heat Transport*

Charney (1971) realized that the heuristic approach to two-dimensional (i.e. barotropic) turbulence was readily extensible to *three*-dimensional quasi-geostrophic turbulence in an unbounded, uniformly rotating, uniformly stratified fluid for which the equation of motion is

$$\left(\frac{\partial}{\partial t} + \mathbf{u}\cdot\nabla\right)\nabla^2\Psi = \text{forcing and dissipation.} \tag{52}$$

In (52) Ψ is now in three dimensions; ∇^2 is the three-dimensional Laplacian in stretched coordinates such that vertical z is replaced by Nz/f, where N is the Väisälä frequency; and $\mathbf{u}$ is horizontal velocity given by $\hat{\mathbf{z}} \times \nabla\Psi$.

Herring (1980) considers both the equilibrium and disequilibrium statistical mechanics of (52). Without forcing or dissipation, motion conserves total enstrophy

$$Q = \overline{q^2} = \sum_{\mathbf{k}} Q_{\mathbf{k}}, \tag{53}$$

where $q = \nabla^2\Psi$ is potential vorticity, $Q_{\mathbf{k}} = q_{\mathbf{k}}q_{-\mathbf{k}}$, and $\mathbf{k}$ refers to the three-dimensional wave vector in the stretched coordinates. Total energy is also conserved as

$$E = \sum_{\mathbf{k}} E_{\mathbf{k}}, \tag{54}$$

where $E_{\mathbf{k}} = Q_{\mathbf{k}}/k^2$ includes both kinetic and available potential energy at $\mathbf{k}$.

Annu. Rev. Fluid Mech. 1986.18:91-147. Downloaded from www.annualreviews.org
by Marine Biological Laboratory - Woods Hole Oceanographic Institution on 04/18/13. For personal use only.

Then just the arguments leading to (29) apply, yielding

$$\langle E_{\mathbf{k}} \rangle = \frac{1}{\alpha_1 + \alpha_2 k^2}. \tag{55}$$

It should be noted that (55) is isotropic in the stretched coordinates and that $E_{\mathbf{k}}$ here is total (not just kinetic) energy.

Disequilibrium study of the three-dimensional quasi-geostrophic evolution under (52) was pursued by Herring (1980) with the goal of discovering to what extent nonlinear transfer enhances the degree of barotropy at larger scales.

Motion fields in the Earth's atmosphere tend to approximate quasi-geostrophy only on the larger scales for which the presence of a rigid lower boundary is significant. In the oceans, however, the quasi-geostrophic approximation may be satisfied on much smaller scales. Although one would not anticipate observing the form (55) on account of forcing and dissipation, oceanic observations at subinertial frequencies tend to support "stretched isotropy" or N/f scaling.

The relation between geostrophic equilibrium (55) and the equilibrium statistics of the full primitive equations has been examined by Errico (1984). Under primitive equations, only energy is a quadratic invariant; hence, one anticipates energy equipartition among all retained modes of both geostrophic and ageostrophic or gravity-wave types. In numerical simulations, Errico observed the evolution as a two-stage process, with an early period of evolution toward the geostrophic equilibrium (55) followed by a more gradual evolution toward energy equipartition among all modes.

The *equilibrium* statistical mechanics of a two-layer quasi-geostrophic system was considered by SHH. The equation of motion is (24) with $i = 1$ and 2 and

$$q_i = \nabla^2 \Psi_i + F_i(\Psi_j - \Psi_i), \tag{56}$$

where $j = 3-i$, $F_i = f_0^2/g'D_i$, and D_i is the average thickness of layer i. Without forcing or dissipation, and given either closed boundaries or periodic boundary conditions, invariants are total energy

$$\begin{aligned} E &= \overline{|\nabla \Psi_1|^2}/F_1 + \overline{|\nabla \Psi_2|^2}/F_2 + \overline{(\Psi_1 - \Psi_2)^2} \\ &= \sum_{\mathbf{k}} [k^2(|\Psi_{1,\mathbf{k}}|^2 F_1^{-1} + |\Psi_{2,\mathbf{k}}|^2 F_2^{-1}) + |\Psi_{1,\mathbf{k}} - \Psi_{2,\mathbf{k}}|^2] \end{aligned} \tag{57}$$

and total enstrophy in each layer

$$Q_i = \overline{q_i^2} = \sum_{\mathbf{k}} |k^2 \Psi_{i,\mathbf{k}} + F_i(\Psi_{j,\mathbf{k}} - \Psi_{i,\mathbf{k}})|^2. \tag{58}$$

Maximum-entropy distributions for $\Psi_{1,\mathbf{k}}$ and $\Psi_{2,\mathbf{k}}$ subject to constraints

Annu. Rev. Fluid Mech. 1986.18:91-147. Downloaded from www.annualreviews.org
by Marine Biological Laboratory - Woods Hole Oceanographic Institution on 04/18/13. For personal use only.

E, Q_1, and Q_2, with arbitrary assignments of F_1 and F_2, are given by SHH. The algebra may be considerably simplified if attention is limited to the case of equal layer depths (hence $F_1 = F_2 = F$). This restriction is not necessary but does render more intuitive the results, which are readily seen as extensions from the one-layer case. For the equal layers, it is convenient to substitute

$$\Psi = (\Psi_1 + \Psi_2)/2, \qquad \tau = (\Psi_1 - \Psi_2)/2, \tag{59}$$

so that Ψ is the barotropic or transport stream function and τ is a vertically averaged buoyancy (and hence is temperaturelike). Defining barotropic and baroclinic modal energies as

$$U_{\mathbf{k}} \equiv k^2|\Psi_{\mathbf{k}}|^2, \qquad V_{\mathbf{k}} \equiv (k^2 + k_R^2)|\tau_{\mathbf{k}}|^2, \tag{60}$$

absolute equilibria (after SHH) simplify to

$$\langle U_{\mathbf{k}} \rangle = \frac{1}{\alpha_1 + \alpha_2 k^2}, \qquad \langle V_{\mathbf{k}} \rangle = \frac{1}{\alpha_1 + \alpha_2 (k^2 + k_R^2)}, \tag{61}$$

where $k_R^2 = 2F$. The expression for $U_{\mathbf{k}}$ is just as with the one-layer equilibrium (29).

It may be seen from (61) that for large $k^2 > k_R^2$, there is approximate equipartition between barotropic and baroclinic energies. However, at small $k^2 < k_R^2$, $V_{\mathbf{k}}$ tends toward a constant value, whereas $U_{\mathbf{k}}$ (for geophysically appropriate α_1 and α_2) tends toward further increase with decreasing k^2. This is much the same surprising conclusion as that seen in Sections 5.3 and 5.4: the condition of maximum entropy is characterized by very well ordered (here depth-independent) flow at the large scales. Numerical-simulation results agree closely with the theoretical result implied by (61). Such a tendency toward barotropy is observed, as discussed, for example, by Rhines (1979).

The tendency toward large-scale barotropy in layered flow may be reconciled with the three-dimensional "stretched isotropy" (55). Essentially k_R^{-1} is just the largest horizontal length scale at which the three-dimensional potential vorticity q can satisfy N/f scaling. At larger horizontal scales, "stretched isotropy" is prevented by the imposition of rigid boundaries.

The *disequilibrium* statistical mechanics of layered flow have been treated by Salmon (1978, 1980), with further discussion by Hoyer & Sadourny (1982) and by Salmon (1982b,c). A restriction to equal layer depths permits an especially simple account even apart from quantitative details of a closure calculation. Salmon (1978) points out that for each triad of wave vectors satisfying $\mathbf{k} + \mathbf{p} + \mathbf{q} = 0$, interactions are constrained to satisfy

$$\dot{U}_{\mathbf{k}} + \dot{U}_{\mathbf{p}} + \dot{U}_{\mathbf{q}} = 0, \qquad k^2 \dot{U}_{\mathbf{k}} + p^2 \dot{U}_{\mathbf{p}} + q^2 \dot{U}_{\mathbf{q}} = 0 \tag{62}$$

Annu. Rev. Fluid Mech. 1986.18:91-147. Downloaded from www.annualreviews.org
by Marine Biological Laboratory - Woods Hole Oceanographic Institution on 04/18/13. For personal use only.

and

$$\dot{U}_{\mathbf{k}} + \dot{V}_{\mathbf{p}} + \dot{V}_{\mathbf{q}} = 0, \qquad k^2\dot{U}_{\mathbf{k}} + (p^2 + k_R^2)\dot{V}_{\mathbf{p}} + (q^2 + k_R^2)\dot{V}_{\mathbf{q}} = 0, \tag{63}$$

where overdots indicate time derivatives. For the barotropic triads UUU, Equations (62) are identical to those of two-dimensional or one-layer turbulence, whose behavior has been extensively studied. It has been noted that constraints upon UUU triads are such as to retain energy in large scales of motion and to tend toward transfer to yet larger scales. These constraints are broken by UVV triads because of the role of k_R. In particular, for $k^2 \approx p^2 \lesssim k_R^2 \gg q^2$, triads of type UVV support the classically studied "baroclinic instability" in which large-scale baroclinic energy $V_{\mathbf{q}}$ may be transferred to smaller-scale baroclinic and barotropic energies $V_{\mathbf{p}}$ and $U_{\mathbf{k}}$. Wave-number local ($k^2 \approx p^2 \approx q^2 \approx k_R^2$) triads of type UVV may then "occlude" or convert baroclinic to barotropic energy, which is subsequently transferred to larger scales under UUU triads.

Closure calculations for the joint evolution of U and V were performed by Salmon (1978) to reveal quantitative details of the UUU and UVV interactions just described; these calculations yielded results in agreement with previous numerical experiments and inferences by Rhines (1977). In this, Salmon achieved a synthesis between classical baroclinic instability analyses and a theory of fully developed turbulence. However, the problem considered assumed statistically isotropic large-scale baroclinic energy and constant Coriolis parameter.

A more difficult problem is posed when one prescribes a horizontally uniform flow with mean vertical shear such that the upper layer translates westward at a rate S faster than a uniform translation of the lower layer. By geostrophy, S is proportional to a mean meridional gradient of depth-averaged temperature. Horizontal anisotropy in eddy statistics must be considered, and Salmon (1980) adopts an angular harmonic expansion after Herring (1975). Since anisotropy is already included, Salmon further includes variation of Coriolis parameter in β-plane approximation. Equal layer depths are assumed, as in Salmon (1978). However, since a coefficient of surface Ekman drag is assumed in the lower layer, the layers are not statistically identical and difference variance arises, which may be expressed as

$$D_{\mathbf{k}} = k^2 \operatorname{Re} \Psi_{\mathbf{k}} \tau_{-\mathbf{k}}. \tag{64}$$

Importantly, a correlation determining the meridional eddy heat flux, with corresponding conversion from mean-flow energy to eddy energy, now occurs and is given by

$$I_{\mathbf{k}} = -k^2 \operatorname{Im} \Psi_{\mathbf{k}} \tau_{-\mathbf{k}}. \tag{65}$$

The closure calculation here becomes most tedious, involving com-

Annu. Rev. Fluid Mech. 1986.18:91-147. Downloaded from www.annualreviews.org
by Marine Biological Laboratory - Woods Hole Oceanographic Institution on 04/18/13. For personal use only.

plicated expressions for the co-evolution of $U_{\mathbf{k}}$, $V_{\mathbf{k}}$, $D_{\mathbf{k}}$, and $I_{\mathbf{k}}$. There occurs moreover a difficulty in principle—namely, that the determination of the coefficient matrix μ leading to (22) is ambiguous, especially if the mean flow is such as to support linearized instability. Somewhat arbitrarily, Salmon (1980) adopted $\theta_{\mathbf{kpq}}$ from (35) as a triad-interaction time scale. It is remarked that the calculated results are not strongly sensitive to specification of $\theta_{\mathbf{kpq}}$. Salmon (1980) further carried out an extensive sequence of direct numerical experiments that were compared with closure calculations; some of the results are shown in Figure 6. Similar results have been reported from numerical experiments by Haidvogel & Held (1980).

Eddy heat flux is an illustration in which the closure calculation is both tedious and, in part, uncertain. In comparison, the numerical empirical approach may be more straightforward and more confident if the problem is one such as "For given S, find the statistically stationary I_k." However, for each different S, β, k_R, or friction, a new I_k would be found by another numerical experiment (or experiments if ensemble averaging were intended). On the other hand, closure expressions, though complicated, are written algebraically and thus admit possible systematic approximation procedures. Salmon (1980) has sought such a simplifying approximation for I_k by writing

$$\dot{I}_k = \text{linear terms} + \text{nonlinear terms} + \text{friction}, \tag{66}$$

where the linear terms are straightforward:

$$\begin{aligned}\text{linear terms} = &-[k_x\beta k_R^2/k^2(k^2+k_R^2)]D_{\mathbf{k}} \\ &+k_xSV_{\mathbf{k}}+k_xS(k_R^2-k^2)(k_R^2+k^2)^{-1}U_{\mathbf{k}}.\end{aligned} \tag{67}$$

After evaluating the full closure expressions for nonlinear terms, Salmon (1980) found some terms to be small and others to be nearly canceling, such that contributions tending to dominate I_k are derived from triads such as $q^2 \ll k^2 \approx p^2$. Expanding in powers of small q^2/k^2 leads to a diffusion-type approximation:

$$\text{nonlinear terms} \approx \theta(k,k,0)\frac{\pi}{4}\,\Omega\left[\frac{1}{k}\frac{\partial}{\partial k}k^3\frac{\partial I}{\partial k}-3I\right], \tag{68}$$

where $\Omega = \int_0^{\varepsilon k} dq\, q^3U(q)$, and k and q refer to continuous wave numbers.

5.7 *"Equatorial Funneling"*

Consider quasi-geostrophic flow with stratification $N(z)$ and nonuniform Coriolis parameter $f(y)$. We may rewrite the equilibrium spectrum (55) as

$$\langle E_{\mathbf{k},n}\rangle = \frac{1}{\alpha_1+\alpha_2(k^2+k_n^2)}, \tag{69}$$

Annu. Rev. Fluid Mech. 1986.18:91-147. Downloaded from www.annualreviews.org
by Marine Biological Laboratory - Woods Hole Oceanographic Institution on 04/18/13. For personal use only.

Annu. Rev. Fluid Mech. 1986.18:91-147. Downloaded from www.annualreviews.org
by Marine Biological Laboratory - Woods Hole Oceanographic Institution on 04/18/13. For personal use only.

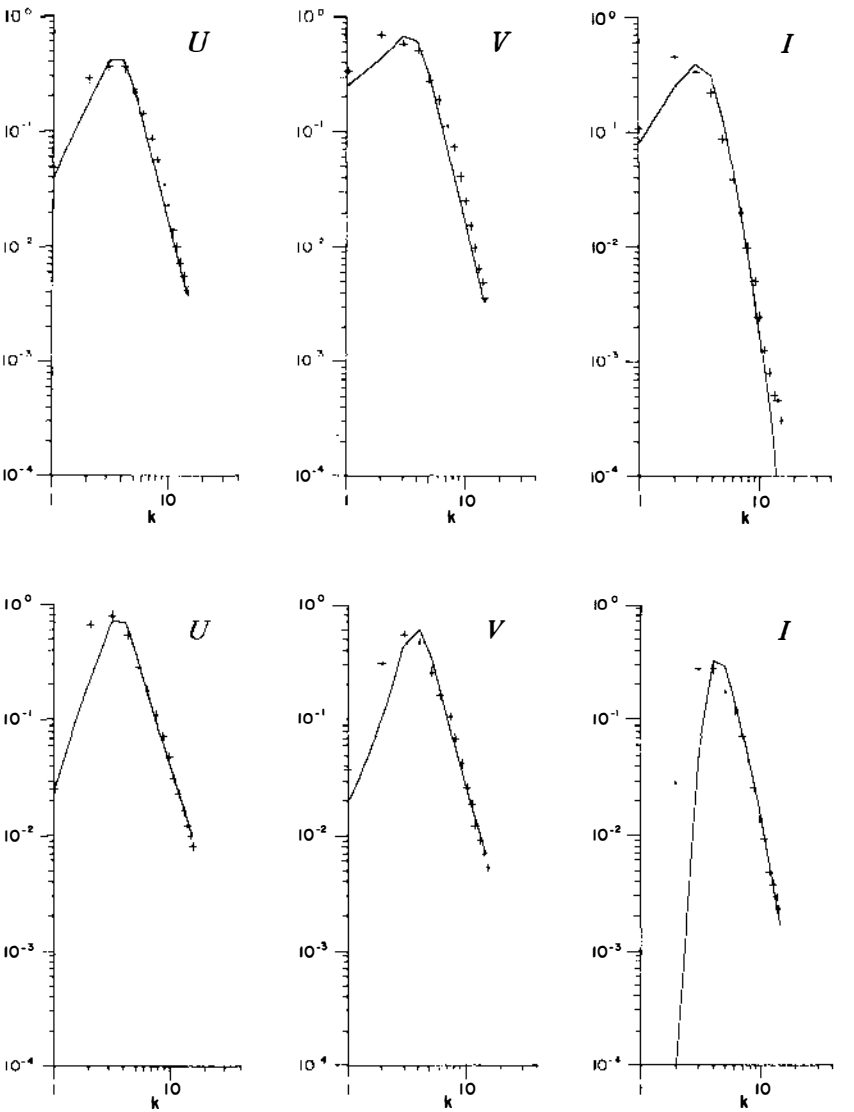

Figure 6 Spectra of barotropic energy $U(k)$, baroclinic energy $V(k)$, and poleward heat flux $I(k)$ are predicted from closure theory (solid curves) and obtained from numerical simulations (crosses). Dissipative, statistically stationary turbulence is maintained by a supercritical mean meridional temperature gradient. Upper panels: $\beta = 0$. Lower panels: $\beta \neq 0$; mean temperature gradient has been increased so as to provide supercriticality (Salmon 1980).

Annu. Rev. Fluid Mech. 1986.18:91-147. Downloaded from www.annualreviews.org
by Marine Biological Laboratory - Woods Hole Oceanographic Institution on 04/18/13. For personal use only.

where $\mathbf{k}$ here is a horizontal rather than a three-dimensional wave vector, n is a vertical mode number, and k_n^{-1} is the nth internal deformation radius. The y-dependence of f enters parametrically through k_n^2, which is an increasing function of n and of f^2. Thus, for given horizontal scale $|\mathbf{k}|^{-1}$, higher vertical modes are expected to have less energy. This tends to be observed. However, the extent to which higher-mode energy is depressed depends upon f^2. In particular, as $f^2 \to 0$, one has $k_n^2 \to 0$ for all n. The implication is that as one approaches the equator, higher vertical modes become relatively increasingly energetic, although quasi geostrophy begins to fail. Indeed, Luyten & Swallow (1976) document the surprising amount of low-frequency energy in high vertical modes in the near-equatorial ocean. Salmon (1982b,c) further explores this "equatorial funneling" effect by employing constant N on an equatorial β-plane and comparing equilibrium statistical theory with direct numerical simulation. The simulation results shown in Figure 7 clearly show the tendency toward accumulation of energy in higher vertical modes near the equator ($y = 0$).

5.8 *Predictability*

By "predictability," we refer to the sensitivity of flow evolution to the precision of initial conditions (Thompson 1957). This issue is one of great importance in relation to practical forecasting of geophysical fields, since (for any given precision of initial condition) forecast skill cannot be improved above a theoretical predictability limit. Research may also be directed toward identifying those areas in which improved resolution of initial conditions might best raise the predictability limit. A number of studies addressing these and related issues are collected in the volume edited by Holloway & West (1984).

Theoretically, the question is posed by considering the evolution of pairs of solutions begun from nearly identical initial conditions. Recalling the discussion in Section 1, we consider pairs of trajectories emerging from a phase volume that is smaller than our presumed resolving power. Denoting the individual trajectories as ζ_1 and ζ_2 with Fourier representation $\zeta_{1,\mathbf{k}}$ and $\zeta_{2,\mathbf{k}}$, we seek to describe the evolution of second-order correlations

$$\begin{aligned} &Z_{\mathbf{k}} \langle \zeta_{i,\mathbf{k}} \zeta_{i,-\mathbf{k}} \rangle, \\ &R_{\mathbf{k}} = \mathrm{Re} \langle \zeta_{i,\mathbf{k}} \zeta_{j,-\mathbf{k}} \rangle, \qquad j = 3-i, \end{aligned} \tag{70}$$

where the ensemble average is over all pairs originating from the prescribed phase volume.

Entropy for the system of pairs follows from (15a):

$$H_2 = \frac{1}{2} \sum_{\mathbf{k}} \ln (Z_{\mathbf{k}}^2 - R_{\mathbf{k}}^2). \tag{71}$$

Annu. Rev. Fluid Mech. 1986.18:91-147. Downloaded from www.annualreviews.org
by Marine Biological Laboratory - Woods Hole Oceanographic Institution on 04/18/13. For personal use only.

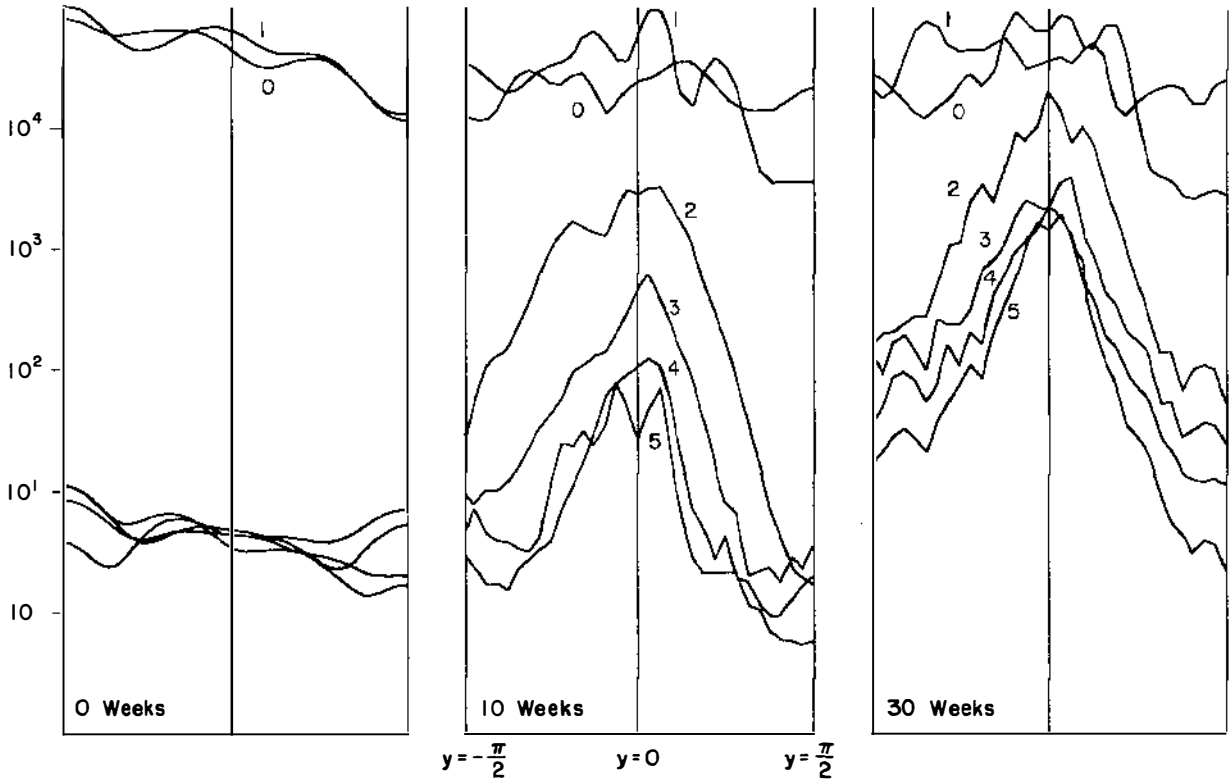

Figure 7 Meridional profiles of kinetic energy in vertical modes $n = 0, 1, 2, 3, 4$, and 5 are shown at 0, 10, and 30 weeks from a numerical simulation of layered quasi-geostrophic motion in an equatorial β-plane ocean. The equator is at $y = 0$. After 30 weeks, high-vertical-mode energy is collected near the equator (Salmon 1982b,c).

Initially the two realizations are highly correlated ($R_{\mathbf{k}} \approx Z_{\mathbf{k}}$) and entropy is small. As time unfolds, trajectories usually will diverge, $R_{\mathbf{k}}$ will diminish, and H_2 will increase for cases where $Z_{\mathbf{k}}$ is stationary. Thus H_2 naturally measures the developing informational uncertainty when, say, ζ_1 is used to forecast ζ_2.

Absolute statistical equilibrium for this problem is a relatively trivial extension of previous results and yields $R_{\mathbf{k}} = 0$ and $Z_{\mathbf{k}} = Z_{\mathbf{k}}^{(eq)}$, where $Z_{\mathbf{k}}^{(eq)}$ is the equilibrium spectrum for each realization ζ_i. In the condition of absolute equilibrium, ζ_i retains no predictive skill relative to, say, ζ_2. Interest in this problem is therefore directed to the question of *approach* to statistical equilibrium, i.e. to the *rate* at which ζ_1 loses predictive value with respect to ζ_2. The problem is then one of disequilibrium statistical mechanics, which may include also the influences of dissipation and of external forcing.

Closure-theoretical models of type (22) have been evaluated for systems of pairs of realizations as expressed in moments (70). Lorenz (1969), Leith (1971), and Leith & Kraichnan (1972) have so treated the case of predictability of two-dimensional turbulence. Numerical simulations by Basdevant et al. (1981), McWilliams & Chow (1981), Vallis (1983), and Holloway (1983b) have extended the earlier results to include the effects of Rossby-wave propagation and of baroclinicity.

Carnevale & Holloway (1982) have considered explicitly the rate of change of entropy (71) in predictability experiments, obtaining

$$\frac{d}{dt} H_2 = \sum_{\mathbf{k},\mathbf{p},\mathbf{q}} \theta_{\mathbf{kpq}} Q_{\mathbf{kpq}}^2 - 2 \sum_{\mathbf{k}} \nu_k + \sum_{\mathbf{k}} \frac{Z_{\mathbf{k}} F_{\mathbf{k}} - R_{\mathbf{k}} W_{\mathbf{k}}}{Z_{\mathbf{k}}^2 - R_{\mathbf{k}}^2}. \tag{72}$$

Here $\theta_{\mathbf{kpq}}$ is a nonnegative quantity that might be given as (35), and $Q_{\mathbf{kpq}}^2$ is a nonnegative expression involving products of $Z_{\mathbf{k}}$ and $R_{\mathbf{k}}$ across the spectrum. Nonnegativity of the first term on the right-hand side of (72) reflects the basic result of Carnevale et al. (1981). Entropy decreases through dissipation, where $\nu_k > 0$ are expansion coefficients of a dissipation operator. External forcing enters through $F_{\mathbf{k}}$ and $W_{\mathbf{k}}$, where $F_{\mathbf{k}}$ is the variance of forcing acting upon $\zeta_{i,\mathbf{k}}$. However, just as we cannot prescribe initial ζ precisely, we possibly cannot prescribe precisely the forcing upon different realizations of ζ. Thus, $W_{\mathbf{k}}$ is taken to be the cross-correlation between forcings of two realizations. If the forcing realizations are uncorrelated, then $W_{\mathbf{k}} = 0$, whereas identical forcing has $W_{\mathbf{k}} = R_{\mathbf{k}}$. In either case external forcing increases H_2, where forcing is considered to derive from an unknown stochastic process.

Derivation of (72) clarified an earlier theoretical dilemma. Usual measures of predictability have consisted of measuring the difference or

Annu. Rev. Fluid Mech. 1986.18:91-147. Downloaded from www.annualreviews.org
by Marine Biological Laboratory - Woods Hole Oceanographic Institution on 04/18/13. For personal use only.

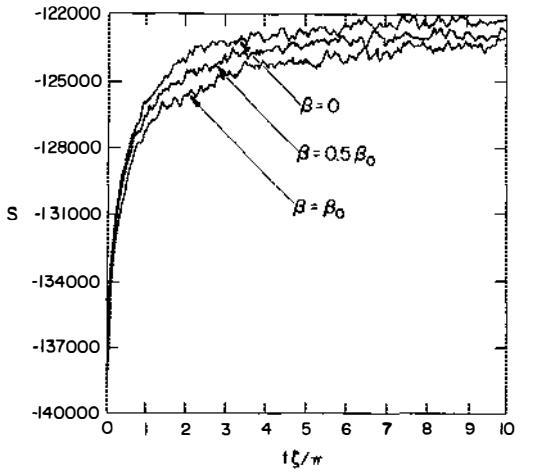

Figure 8 Entropy provides a measure of the degradation of forecast information with increasing forecast period for the case of barotropic motion on a β-plane. Entropy is observed here from specific realizations, and hence it suffers fluctuations, whereas entropy growth would be monotonic on ensemble average for unforced, nondissipative motion. Three values of β are indicated, from $\beta = 0$ up to $\beta = \beta_0$ (approximately terrestrial). It is seen that β suppresses entropy growth, thereby yielding enhanced predictability (Carnevale & Holloway 1982).

distance between two realizations of ζ according to some metric. Resulting measures might be variance of 500-mbar height fields (effectively Ψ), variance of difference velocity, or variance of difference vorticity. A theoretical dilemma was that none of these measures demonstrably satisfied the intuitive property that "uncertainty" should monotonically increase, on average, with increasing time apart from direct influences of forcing or dissipation. Entropy (71) as an information-theoretical measure of uncertainty satisfies the intuitive Second Law expectation. Nonetheless, (71) appears not to be so useful as a measure of forecast skill, since it tends to be dominated by forecast information concerning small scales of motion, as discussed by Carnevale & Vallis (1984).

Evolution of experimental entropy, i.e. (71) as determined from a single pair of realizations rather than as an average over the ensemble of pairs, is shown in Figure 8. Three cases are shown in which β ranges from zero up to a value that is approximately terrestrial. It is seen that larger β suppresses the growth of H_2, enhancing predictability.

5.9 *Stirring of Tracer Fields*

The preceding examples may be extended to include advection of passive tracer fields. By passive, we mean that the tracer concentration has no direct

Annu. Rev. Fluid Mech. 1986.18:91-147. Downloaded from www.annualreviews.org
by Marine Biological Laboratory - Woods Hole Oceanographic Institution on 04/18/13. For personal use only.

influence on the velocity field. The statistical mechanics of the velocity field are therefore unaffected, and we are concerned only with the statistical mechanics of the tracer.

For a tracer concentration field $\phi(\mathbf{x}, t)$ advected by nondivergent, two-dimensional flow, the equation of motion is

$$\frac{\partial}{\partial t}\phi + J(\Psi, \phi + \mathbf{G}\cdot\mathbf{x}) + \mathscr{D}_\phi(\phi) = \mathscr{E}_\phi. \tag{73}$$

Here ϕ is the departure from a large-scale background field $\langle\phi\rangle = \mathbf{G}\cdot\mathbf{x}$, $\mathscr{D}_\phi$ is a dissipation operator, $\mathscr{E}_\phi$ is any external source for ϕ, and Ψ is the stream function from a velocity field that might satisfy (24), for example.

In the simplest case, we consider (73) with $\mathbf{G} = \mathscr{D}_\phi = \mathscr{E}_\phi = 0$ and boundary conditions consisting either of a closed, impermeable basin or of periodicity for Ψ- and ϕ-fields. Spectrally truncated equations conserve $\overline{\phi^2}$ and $\overline{\phi q}$, where q is potential vorticity under the assumption that $\mathscr{D} = \mathscr{E} = 0$ in (24). In particular, if we consider the uncorrelated case $\overline{\phi q} = 0$, then absolute statistical equilibrium is simply equipartition

$$\Phi_{\mathbf{k}} = \langle\phi_{\mathbf{k}}\phi_{-\mathbf{k}}\rangle = C \tag{74}$$

independent of the statistical distribution of the advecting velocity field that brings about (74)!

Even in this simplest case, one may entertain an apparent paradox. Consider an unforced, nondissipative evolution from initial conditions in which ϕ and q are given identical probability distributions. Fields ϕ and q only evolve under advection by the same stream function Ψ. One might therefore suppose that distributions of ϕ and q will evolve similarly. On the other hand, evolution of q is constrained by conservation of energy as well as of $\overline{q^2}$, and so q should evolve to a statistical distribution different from that of ϕ. Evolution from identical initial probability distributions to different equilibrium distributions is indeed what happens, as seen in Figure 9.

The *disequilibrium statistical mechanics* of tracer stirring in statistically homogeneous, isotropic, two-dimensional turbulence have been considered by Lesieur et al. (1981) and by Lesieur & Herring (1985), with the latter authors considering also the case with tracer-vorticity correlation $\overline{\phi\zeta} \neq 0$. Introduction of β induces anisotropy in the vorticity field (as discussed in a previous illustration). However, the effect of β is even more marked with respect to the tracer field. This is seen both in numerical simulations (Haidvogel & Keffer 1984) and in theory (Holloway & Kristmannsson 1984). In addition to β, one may also impose a uniform background gradient $\mathbf{G}$ in the tracer concentration, which allows investigation of the phenomenon of net turbulent transport of tracer substance.

Annu. Rev. Fluid Mech. 1986.18:91-147. Downloaded from www.annualreviews.org
by Marine Biological Laboratory - Woods Hole Oceanographic Institution on 04/18/13. For personal use only.

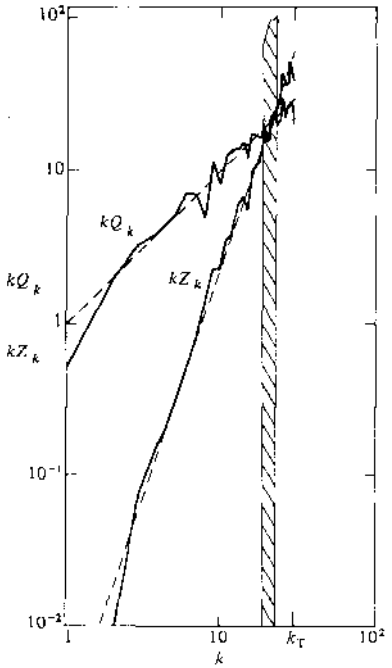

Figure 9 Spectra of tracer variance and of vorticity variance illustrate the evolution of unforced, nondissipative flow. One-dimensional spectra shown in the figure are the sums of modal variances $\Phi_{\mathbf{k}}$ and $Z_{\mathbf{k}}$ in circular wave bands of radius $k = |\mathbf{k}|$. Initial spectra of tracer ($\Phi_{\mathbf{k}}$) and of vorticity ($Z_{\mathbf{k}}$) are identical (shown shaded). At a later time, $\Phi_{\mathbf{k}}$ and $Z_{\mathbf{k}}$ (shown as solid curves) have approached their separate equipartition or maximum-entropy solutions (shown as dashed curves) (Holloway & Kristmannsson 1984).

The mean spatial flux of substance is given by

$$\langle \mathbf{u}\phi \rangle = \sum_{\mathbf{k}} \frac{\mathbf{k} \times \hat{\mathbf{z}}}{k^2} \operatorname{Im} \Gamma_{\mathbf{k}}, \tag{75}$$

where $\Gamma_{\mathbf{k}} = \langle \zeta_{\mathbf{k}} \phi_{-\mathbf{k}} \rangle$. Disequilibrium evolution of $\Phi_{\mathbf{k}}$ and $\Gamma_{\mathbf{k}}$ is then given by Holloway & Kristmannsson (1984) as

$$\left(\frac{d}{dt} + 2\kappa_k + 2\gamma_{\mathbf{k}}\right)\Phi_{\mathbf{k}} = Q_{\mathbf{k}} - \frac{2\hat{\mathbf{z}} \cdot (\mathbf{G} \times \mathbf{k})}{k^2} \operatorname{Im} \Gamma_{\mathbf{k}} \tag{76a}$$

and

$$\left(\frac{d}{dt} + i\omega_{\mathbf{k}} + \nu_k + \kappa_k + \eta_{\mathbf{k}} + \gamma_{\mathbf{k}}\right)\Gamma_{\mathbf{k}} = -i \frac{\hat{\mathbf{z}} \cdot (\mathbf{G} \times \mathbf{k})}{k^2} Z_{\mathbf{k}}, \tag{76b}$$

where $\gamma_{\mathbf{k}}$ and $\eta_{\mathbf{k}}$ are expressions given by weighted sums over spectra of ζ only, while $Q_{\mathbf{k}}$ involves products of spectra of ζ and of ϕ. Also, κ_k is the transform of the dissipation operator $\mathscr{D}_\phi$, and ν_k is the transform of dissipation acting on the vorticity field. Wave dispersion such as (36) appears explicitly as $i\omega_{\mathbf{k}}$ in (76b). Equations (76a,b) are evaluated together with an equation such as (34) for the evolution of the vorticity spectrum.

Annu. Rev. Fluid Mech. 1986.18:91-147. Downloaded from www.annualreviews.org
by Marine Biological Laboratory - Woods Hole Oceanographic Institution on 04/18/13. For personal use only.

An item to note is that **G** appears as the inhomogeneous part of (76b), in which quantities $\gamma_{\mathbf{k}}$ and $\eta_{\mathbf{k}}$ do not depend upon $\Phi_{\mathbf{k}}$ or $\Gamma_{\mathbf{k}}$ and are thus independent of **G**. The result is that the statistically stationary, *disequilibrium* solution for $\Gamma_{\mathbf{k}}$ is linearly dependent upon **G**. Consequently we may express (75) as

$$\langle \mathbf{u}\phi \rangle = -\left(\sum_{\mathbf{k}} \mathbf{D}_{\mathbf{k}} \right) \cdot \mathbf{G}, \tag{77}$$

where $\mathbf{D}_{\mathbf{k}}$ are spectral contributions to an overall "eddy diffusivity" tensor **D**.

"Eddy diffusivity" is a popular notion in many practical applications but is usually perforce introduced in an ad hoc, often suspect, manner. The development given above permits systematic theoretical derivation of **D**. In particular, Holloway & Kristmannsson (1984) examine the role of β in inducing anisotropy into **D** such that meridional diffusivity D_{yy} may be greatly reduced relative to the zonal diffusivity D_{xx}. The theoretical results concerning anisotropic **D** were demonstrated to emerge as well in numerical experiments.

A very important remark should be made here. What we have just described is a systematic derivation of eddy diffusivity **D** as regards a passive tracer. This must not be construed as lending broader support to ad hoc application of eddy-diffusion ideas. In particular, one ought to be cautioned against the very popular idea that eddies necessarily support down-gradient mixing of potential vorticity (Green 1970, Welander 1973, Rhines & Young 1982).

Indeed this illustration provides a clear counterexample. A meridional component of **G** will drive a meridional transport of passive tracer (i.e. the eddies exhibit $D_{yy} > 0$ with respect to the tracer). For the same problem, β is the meridional gradient of q that one might imagine driving a meridional vorticity flux. However, in the absence of an external source for mean momentum, nonzero meridional vorticity flux would violate zonal momentum balance. Thus we observe that the same eddies that support down-gradient tracer transport are unable to transport potential vorticity. In other circumstances, gradient transports of vorticity may occur; the point emphasized here is that ad hoc supposition of gradient transport of vorticity is a haphazard proposition.

Differences between vorticity and a passive tracer are also seen in their transport in **k**-space. Recall the systematic differences that appeared between passive tracer and vorticity with regard to absolute *equilibrium* (cf. Figure 9). Corresponding differences can be identified in the *disequilibrium* evolution of the two fields. Holloway & Kristmannsson (1984) demonstrated that the coefficient $\gamma_{\mathbf{k}}$ in the passive-tracer variance equation

Annu. Rev. Fluid Mech. 1986.18:91-147. Downloaded from www.annualreviews.org
by Marine Biological Laboratory - Woods Hole Oceanographic Institution on 04/18/13. For personal use only.

(76a) is systematically larger than a coefficient η_k that occurs in vorticity-variance equations. This results in more efficient transfer of passive-tracer variance to small scales. A visual display of the difference in behavior is shown in Figure 10 from a numerical simulation. The cause of the difference is wave-number local interactions, which are most efficient at transferring passive-tracer variance but which become vanishingly inefficient at transferring vorticity variance under the idealization of two-dimensional geometry. The different behavior is also evident at large scales, for which two-dimensional turbulence tends to produce a reverse cascade of kinetic energy toward still larger scales yielding asymptotically a kinetic-energy spectrum as $k^{-5/3}$ (Kraichnan 1967). On the same large scales, classical arguments since Obukhov's (1949) discussion apply; these indicate a direct cascade of tracer variance toward smaller scales with a tracer-variance spectrum also asymptotically approaching $k^{-5/3}$. On the same subrange, tracer and velocity variances cascade in opposite directions! The dominant transfer mechanisms on such scales tend to be fairly local in wave number. Only for widely scale-disparate interactions such that small-scale features are strained directly by large-scale flow is it admissible to consider vorticity approximately as a passive tracer.

5.10 *Plankton Patchiness*

An extension from the preceding section is to consider the role that horizontal advection plays in maintaining the patchiness of the field of primary productivity in the upper ocean. In fact a vast wealth of biological dynamics and of vertical exchange processes are believed to be involved. However, it is interesting to consider to what extent horizontal differential advection might dominate other sources of variability.

Consider only the simplest kind of biological dynamics, consisting of exponential increase or decrease of populations. Let $\phi(\mathbf{x}, t)$ be the vertical integral of the logarithm of biomass concentration. Logarithms are useful here both because concentration is nonnegative and because actual populations are observed to be approximately lognormally distributed. Let the vertically integrated horizontal velocity in the upper ocean be described by a transport stream function Ψ. Then a plausible model for evolution of ϕ is (73), where $\mathscr{E}_\phi(\mathbf{x}, t)$ is taken to be the vertical integral of the rate coefficient for exponential increase or decrease. Effects of vertical shear in the velocity field are not included explicitly but are treated as a shear-dispersion effect (Kullenberg 1972, Young et al. 1982) expressed as a diffusion $\mathscr{D}_\phi$.

If we consider $\mathscr{E}_\phi$ to be some random field with prescribed spatial and temporal statistics, then, given the statistical evolution of Ψ, we seek the statistical evolution of ϕ. Forcing on account of the biological dynamics $\mathscr{E}_\phi$ and dissipation by shear dispersion $\mathscr{D}_\phi$ are essential, so that only the *disequilibrium* treatment is of interest.

Annu. Rev. Fluid Mech. 1986.18:91-147. Downloaded from www.annualreviews.org
by Marine Biological Laboratory - Woods Hole Oceanographic Institution on 04/18/13. For personal use only.

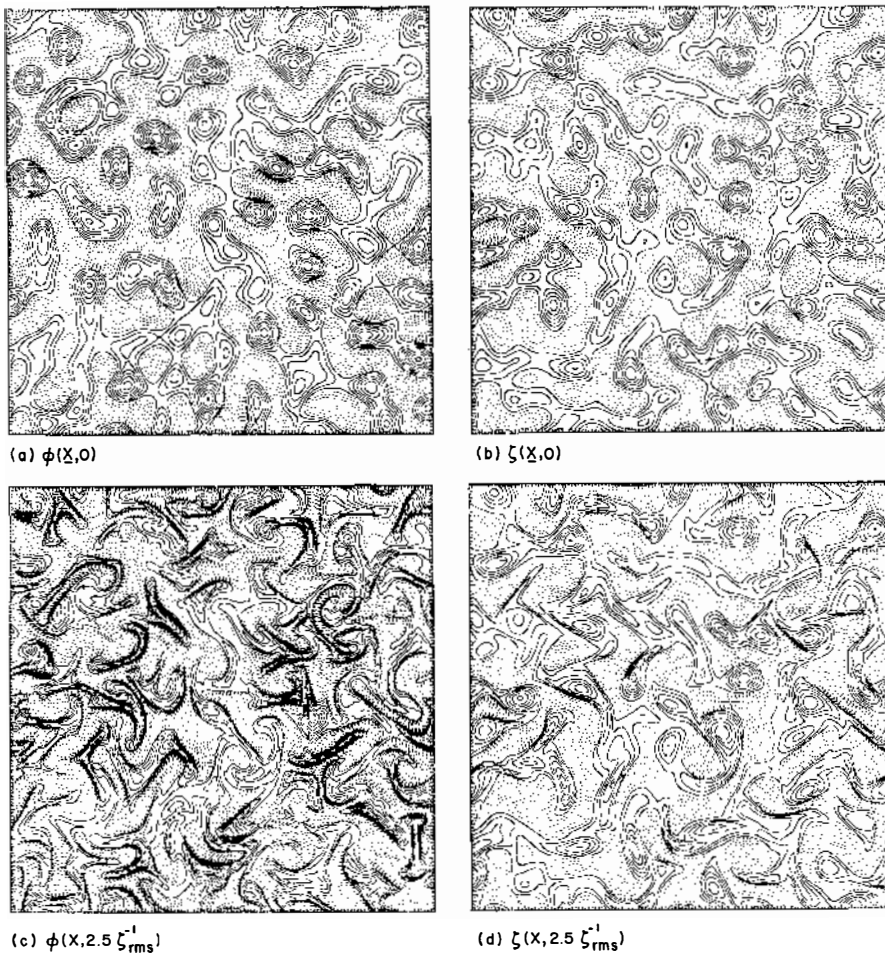

Figure 10 Spatial fields of passive tracer ϕ and vorticity ζ are shown from a spinning-down numerical experiment. At $t = 0$ (*a*, *b*) the two fields have identical spectral distributions. At a later time (*c*, *d*) the passive-tracer field has evolved higher-wave-number features than the vorticity field. Thus it is hazardous to think of vorticity as a passive tracer (Holloway & Kristmannsson 1984).

Suppose that $\mathscr{E}_\phi$ has structure only on large scales, i.e. $\mathscr{E}_\phi$ has variance only for, say, $k < k_1$. The temporal variability of $\mathscr{E}_\phi$ is another matter; we may consider two extremes:

1. $\mathscr{E}_\phi$ changes randomly over time scales that are short compared with eddy-advection time scales.
2. $\mathscr{E}_\phi$ is constant over time.

Annu. Rev. Fluid Mech. 1986.18:91-147. Downloaded from www.annualreviews.org
by Marine Biological Laboratory - Woods Hole Oceanographic Institution on 04/18/13. For personal use only.

The extremes are selected because they span the range of interesting time dependences and because each is tractable under closure theory.

Case 1 yields essentially (76a) without **G**:

$$\left(\frac{d}{dt} + 2\kappa_k + 2\gamma_{\mathbf{k}}\right)\Phi_{\mathbf{k}} = Q_{\mathbf{k}} + S_{\mathbf{k}}, \tag{78}$$

where each of the terms is as previously (for details, see Holloway & Kristmannsson 1984) except for the inclusion of $S_{\mathbf{k}}$, which is the variance of the temporal fluctuations in $\mathscr{E}_\phi$.

Case 2 requires that we consider the cross-correlation $\Lambda_{\mathbf{k}} = \langle \phi_{\mathbf{k}} r_{-\mathbf{k}} \rangle$ between the plankton burden ϕ and the "frozen" rate-coefficient field $\mathscr{E}_\phi(\mathbf{x}, t) = r(\mathbf{x})$. Closure equations are

$$\left(\frac{d}{dt} + 2\kappa_k + 2\gamma_{\mathbf{k}}\right)\Phi_{\mathbf{k}} = Q_{\mathbf{k}} + \Lambda_{\mathbf{k}}, \tag{79a}$$

$$\left(\frac{d}{dt} + \kappa_k + \gamma_{\mathbf{k}}\right)\Lambda_{\mathbf{k}} = \hat{S}_{\mathbf{k}} = \langle r_{\mathbf{k}} r_{-\mathbf{k}} \rangle. \tag{79b}$$

Numerical experiments have been performed by D. Ramsden (unpublished) for cases 1 and 2 and have been compared with a theoretical evaluation using (78) and (79). Some of these results are seen in Figure 11. We have posed the plankton-patchiness question in terms of the horizontal wave-number spectrum of the logarithm of plankton burden. For the simple biological dynamics assumed here, it is seen that there is agreement between theory and numerical experiment for the shape of the spectrum and the growth dynamics, nonlinear transfer, and shear dispersion that maintain that spectrum.

It may be noteworthy that certain questions about patchiness can be answered from (78) and (79) by inspection. For example, it has been speculated that the very different time dependences assumed for $\mathscr{E}_\phi$ in cases 1 and 2 might lead to very different characteristics of patchiness. However, in terms of the shape of spectrum $\Phi_{\mathbf{k}}$, such differences are slight. If we assume approximate statistical stationarity, then $\Lambda_{\mathbf{k}}$ from (79b) is $\hat{S}_{\mathbf{k}}/(\kappa_k + \gamma_{\mathbf{k}})$. If $\hat{S}_{\mathbf{k}}$ is given the same form as $S_{\mathbf{k}}$, then $\Lambda_{\mathbf{k}}$ on the right-hand side of (79a) will be more red than will $S_{\mathbf{k}}$ in (78) when it is taken into account that $\kappa_k + \gamma_{\mathbf{k}}$ tend to be increasing functions of k. Therefore, in case 2, $\Phi_{\mathbf{k}}$ will be slightly more red on the scales subject to direct biological forcing. Over all k not directly forced, $S_{\mathbf{k}}$ and $\Lambda_{\mathbf{k}}$ vanish and no discernible difference between cases 1 and 2 is expected. Numerical simulations have been performed that indeed demonstrate no significant difference between cases 1 and 2 as regards the shape of $\Phi_{\mathbf{k}}$ over scales not directly forced.

Annu. Rev. Fluid Mech. 1986.18:91-147. Downloaded from www.annualreviews.org
by Marine Biological Laboratory - Woods Hole Oceanographic Institution on 04/18/13. For personal use only.

Annu. Rev. Fluid Mech. 1986.18:91-147. Downloaded from www.annualreviews.org
by Marine Biological Laboratory - Woods Hole Oceanographic Institution on 04/18/13. For personal use only.

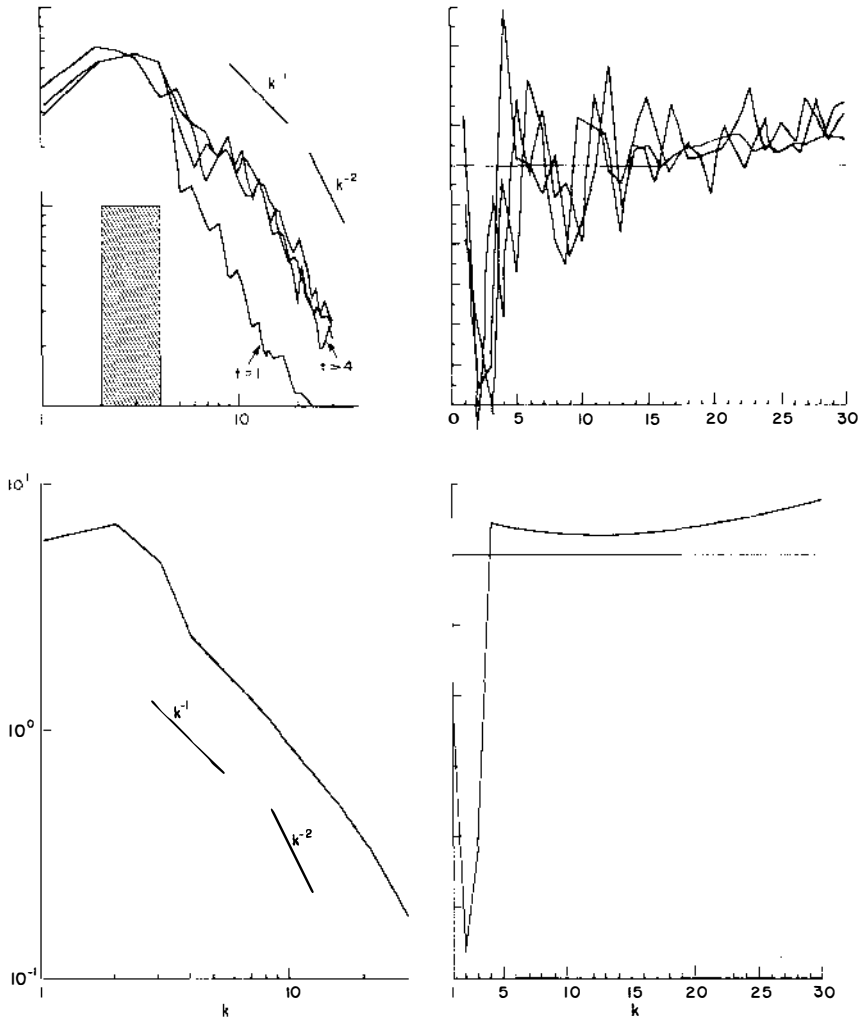

Figure 11 Horizontal wave-number spectra of plankton patchiness are compared from numerical simulations and from closure theory. Case 2, in which random rate coefficient field $\mathscr{E}_\phi$ is constant in time, is considered here. Upper panels: Plankton spectra from numerical experiments are shown at successive times, becoming essentially stationary after a nominal time $t = 4$. The spectrum of the rate field $\mathscr{E}_\phi$ is shown hatched. Instantaneous traces of the turbulent transfer function $T(k)$ are shown. Lower panels: Stationary spectra and transfer function are evaluated from closure theory using (79). In this figure, $T(k) > 0$ indicates turbulence providing a source of patchiness variance at wave number k; $T(k) < 0$ indicates turbulence removing variance. The simple balance is that "biological dynamics" $\mathscr{E}_\phi$ is here assumed to generate patchiness at large length scale (low k), which is transferred by turbulence to short length scales where variance is dissipated by explicitly modeled diffusion (D. Ramsden, unpublished).

5.11 *Internal Gravity Waves/Buoyant Turbulence*

A final illustration is included to demonstrate different space and time scales and different dynamics that are amenable to the statistical-mechanics approach. A most striking observation, first suggested by Garrett & Munk (1972), is that internal oceanic fluctuating fields on length scales from $O(10\text{ m})$ to $O(1000\text{ m})$ and time scales from the inertial frequency f to the buoyancy frequency N exhibit remarkably reproducible variance spectra from many different locations in different oceans during different seasons. If the fluctuating fields are attributed to a random superposition of internal inertial-gravity waves, then the result is to observe a seemingly "universal" spectrum of internal-wave variance, commonly denoted the GM spectrum. In fact, some departures from universality are observed. The problem is being actively researched and is discussed in recent reviews by Garrett & Munk (1979), Munk (1981), and Olbers (1983); page space requires that the present recount be extremely superficial as regards the observations.

The GM spectral model assumes linearized internal-wave modes, to which a variance spectrum is empirically fit. No further dynamics are assumed in setting the empirical form of the variance spectrum. This empirical form has evolved through a number of revisions and was recently listed by Munk (1981) in terms of vertical modes j of an exponentially stratified ocean as an energy spectrum

$$E(\omega,j) = b^2 N_0 N E_0 B(\omega) H(j) \tag{80}$$

with

$$B(\omega) = \frac{2}{\pi}\frac{f}{\omega}(\omega^2 - f^2)^{-1/2}, \tag{81a}$$

$$H(j) = H_*(j^2 + j_*^2)^{-1}, \tag{81b}$$

where b is a scale depth of 1.3 km, $N_0 = 5.2 \times 10^{-3}\ \text{s}^{-1}$, and E_0 and j_* are fit parameters taking values near $E_0 = 6 \times 10^{-6}$, $j_* = 3$. A depth-dependent vertical wave number may be assigned to j under WKB approximation as $k_z = jN(z)/bN_0$. On the assumption that underlying dynamics are linearized waves [hence satisfying precisely a dispersion relation $\omega = \pm\Omega(k_h, j)$], and with a further ad hoc assumption of statistical isotropy in the horizontal, one may convert spectral density in (ω,j) as in (80) into spectral density in (k_h, k_z).

The intriguing property of (80) is that it is specified not only in form but also in absolute amplitude per E_0. (One is cautioned that this result is empirical and hence subject to continuing update.) Reproducibility of (80) has attracted a great deal of theoretical attention.

Annu. Rev. Fluid Mech. 1986.18:91-147. Downloaded from www.annualreviews.org
by Marine Biological Laboratory - Woods Hole Oceanographic Institution on 04/18/13. For personal use only.

Annu. Rev. Fluid Mech. 1986.18:91-147. Downloaded from www.annualreviews.org
by Marine Biological Laboratory - Woods Hole Oceanographic Institution on 04/18/13. For personal use only.

An overall account of the oceanic internal-wave field would entail analyses of forcing and dissipation mechanisms (cf. the reviews cited above). However, a simple remark is that apparent energetic sources are nonuniformly distributed in space or in time, and thus do not simply account for the universality of (80).

An early consideration was whether the GM spectrum might represent an *equilibrium* distribution. Observed internal dissipation rates in the ocean are highly intermittent but tend to be small, yielding estimates of energy residence times of $O(10$ days). Perhaps such times would permit an approach to absolute equilibrium. Nondissipative invariants of the motion are total energy and net horizontal wave momentum. Under horizontal isotropy, net momentum vanishes, leaving only the energy invariant. Then simple energy equipartition would anticipate spectral density

$$E(k_h, k_z) \propto k_h, \tag{82}$$

where k_h is the magnitude of the horizontal wave vector.

One sees that (82) is far from (80). Most investigators have therefore sought to explain (80) by including essential roles of forcing and dissipation. However, Allen & Joseph (1985a) have examined the detailed dynamics leading to absolute equilibrium among internal waves. Depending upon how one elects to impose high-wave-number cutoffs to prevent ultraviolet catastrophe, Allen & Joseph show that some marginal spectra calculated from (82) may resemble some of the observations from which (80) was constructed. Nonetheless, other significant discrepancies remain. Moreover, these considerations have not taken account of a spectrum of geostrophic turbulence [cf. (55)], which would be in equilibrium with the internal-wave spectrum. Further efforts by Allen & Joseph (1985b) seek to address this question. (See also Errico (1984), as discussed in Section 5.6.)

Much greater effort has been expended in exploring a *disequilibrium* account. Here there was hope, based upon the GM assumption of underlying linearized wave dynamics, that one might proceed perturbatively in smallness of wave amplitude. Then the spectral evolution might be guided by weak wave resonant-interaction theory [essentially (17) with (20) and (21)]. Detailed calculations of this type have been examined by Müller & Olbers (1975), Olbers (1976), McComas & Bretherton (1977), McComas (1977), and Pomphrey et al. (1980). Analytically derived approximations to the spectral evolution equation are given by McComas & Bretherton (1977) and McComas & Müller (1981a); these provide clearer insight into some of the mechanisms involved and lead to an overall scenario for energy balance as proposed by McComas & Müller (1981b).

However, there are two main reasons to doubt the validity of calculations to date. The first concern is for finite strength of interaction. In usual

derivations, weak wave-interaction theory depends upon multiple time scaling, such that systematic energy transfer is only effected on time scales long compared with the wave period [cf. Benney & Saffman (1966) or Benney & Newell (1969)]. At GM amplitudes, the above-cited calculations appear to violate this premise by anticipating energy transfer on time scales much shorter than the wave period (Holloway 1980). Since this result is self-contradictory, it should not be used to estimate actual interaction time scales. There are further ambiguities concerning the notion of "interaction time," as argued between McComas & Müller (1981a) and Holloway (1982). Moreover, it is not clear that criteria based solely upon wave period are appropriate. Finite-amplitude theory (Holloway 1979) suggests the importance of a "group period" given by a characteristic packet length divided by the group speed, whereas the theory of stochastic differential equations (Van Kampen 1981) indicates the role of a Kubo-number criterion, as further discussed by Müller et al. (1985).

The second concern may prove even more troublesome. It has been recognized for some time that oceanic observations contain fluctuations that are other than internal waves; these are sometimes referred to as "contaminations" (Müller et al. 1978). Laboratory studies (as reviewed by Lin & Pao 1979) and three-dimensional numerical simulations (Riley et al. 1981) show that collapsing, stably stratified turbulence readily sorts into nonlinear internal waves together with quasi-two-dimensional vortices, sometimes called "pancake," "blini," or "vortical" modes. Holloway (1981, 1983a) points out that when one considers incompressible, stably stratified flow including a background component of uniform rotation, a complete eigenfunction representation requires three fields, two of which are the upward- and downward-propagating internal waves, while the third field is geostrophic motion as considered in Section 5.6. The problem is seriously compounded by the necessity of calculating not only energetic exchanges among the internal waves but also exchanges between the geostrophic and internal-wave branches, along with the geostrophic turbulence considered previously. At higher wave numbers, nonlinear interaction will broaden the frequency distributions associated with the separate eigenfunctions, leading to overlapping frequency distributions. This picture is sketched in Figure 12. Here we imagine spectra of internal waves and of geostrophic turbulence entwined on all scales.

The difficulties just described are daunting. As a means of exploring finite-amplitude effects on the purely internal wave-wave interaction, Carnevale & Frederiksen (1983) have considered an idealization in which motion is restricted to lie in a vertical plane and the Earth's rotation is neglected. Equations of motion can then be given in terms of the horizontal

Annu. Rev. Fluid Mech. 1986.18:91-147. Downloaded from www.annualreviews.org
by Marine Biological Laboratory - Woods Hole Oceanographic Institution on 04/18/13. For personal use only.

component $\zeta(x,z,t)$ of a vorticity field and a density-anomaly field $\rho(x,z,t)$:

$$\frac{\partial}{\partial t}\zeta + J(\Psi,\zeta) + \frac{\partial}{\partial x}\rho - \nu\nabla^2\zeta = 0, \tag{83a}$$

$$\frac{\partial}{\partial t}\rho + J(\Psi,\rho) - \frac{\partial}{\partial x}\Psi - \kappa\nabla^2\rho = 0, \tag{83b}$$

where Ψ is the stream function in the vertical (x,z) plane and ∇^2 is the two-

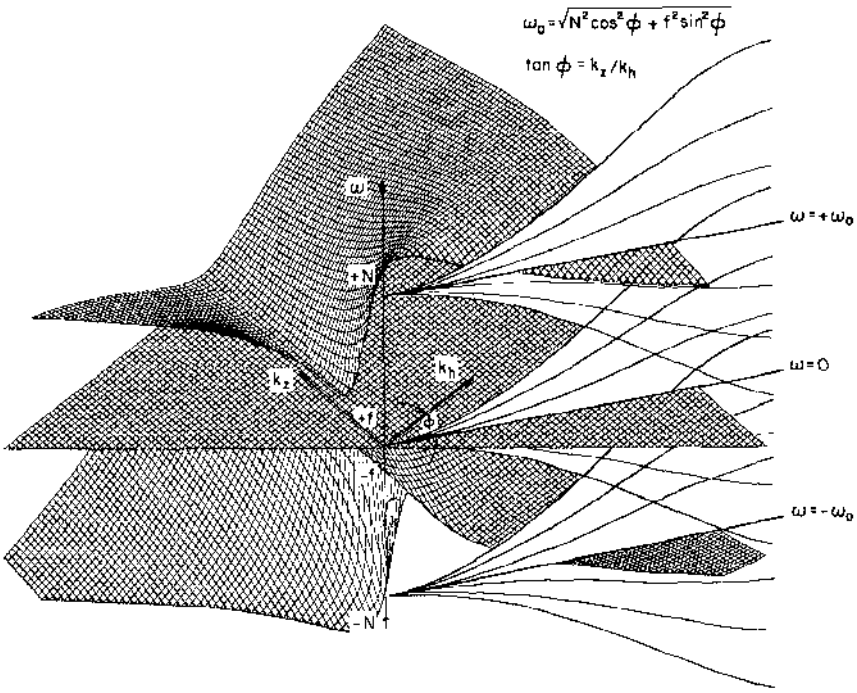

Figure 12 Solution surfaces for the linear dispersion relation $\omega = \pm\Omega$ and the surface $\omega = 0$ are shown as hatched surfaces in ω, k_h, k_z-space. For a particular aspect ratio $k_z/k_h = \tan\phi$, the natural frequencies $\omega = \pm\omega_0$ and $\omega = 0$ are given by the intersection of the dispersion relations (hatched surfaces) and the plane $k_z/k_h = \tan\phi$. These intersections are the straight lines labeled $\omega = +\omega_0$, $\omega = 0$, and $\omega = -\omega_0$. Because of nonlinear interactions, energy will be distributed about the natural frequencies. This relative distribution of energy is sketched as fanlike curves, which may be regarded as contours of relative energy density, decreasing away from the natural frequencies. At large wave numbers, the fans become very broad, with the different branches overlapping. This figure emphasizes the presence of *three* interacting modes at all scales, as well as a continuous transition from more wavelike dynamics at small wave number to more turbulent dynamics at higher wave numbers (Holloway 1983a).

Annu. Rev. Fluid Mech. 1986.18:91-147. Downloaded from www.annualreviews.org
by Marine Biological Laboratory - Woods Hole Oceanographic Institution on 04/18/13. For personal use only.

dimensional Laplacian. Two linearized wave modes are then given by

$$a_{\mathbf{k}}^{\pm} = |k|\Psi_{\mathbf{k}} \pm \rho_{\mathbf{k}}, \tag{84}$$

where $\Psi_{\mathbf{k}}$ and $\rho_{\mathbf{k}}$ are wave-vector expansion coefficients for Ψ and ρ. Carnevale & Frederiksen (1983) then consider both equilibrium and disequilibrium [i.e. closure equations such as (23), differing from weak wave-interaction theory on account of $\mu \neq 0$] distributions for $A_{\mathbf{k}}^{s} = \langle a_{\mathbf{k}}^{s} a^{s}{}_{-\mathbf{k}} \rangle$. Furthermore, Frederiksen & Bell (1983, 1984) have performed numerical simulations of (83), testing the theoretical results from Carnevale & Frederiksen.

6. SUMMARY AND OUTLOOK

The methods reviewed in this paper tend to lie outside the mainstreams of GFD research. Many calculations (not shown explicitly in this review) are complicated and laborious as well as uncertain on some points. A reader may wonder why one ought to bother. There may be two reasons why.

1. The statistical mechanics of macroscale geophysical flows provides a synthesizing *point of view*. Observations of atmospheric and oceanic fields as well as output from high-resolution numerical simulations tend to place us in a role of onlookers in a seemingly chaotic landscape of overlapping/competing flow mechanisms. Explosively mounting volumes of field observations and of simulation output threaten to overwhelm an empirical attitude toward either nature or computer. Statistical mechanics here suggests at least a sense of direction, i.e. we perceive processes of entropy generation and a tendency toward entropy maximization.

2. Point of view, as such, may be only a matter of taste. It is just as important that the methods described here provide a prescription for *quantitative calculation* and that these calculations have been repeatedly *tested* for a variety of problems against empirical results collected from numerical simulations.

Throughout we have sought to compare results from *equilibrium* and *disequilibrium* methods. The two methods are related by entropy, which we understand in terms of probability distributions for macroscale flows. In this we proceed from the view of information theory, noting that entropy as (7) or (8) may be extended to include the specific thermodynamic entropy of the fluid. Novelty is seen in that the same entropy functional accounts for establishment of planetary-scale flow regimes.

Exercise of *equilibrium methods* requires an artificial idealization. We are obliged to represent a continuous flow in a system of finite degrees of freedom while neglecting external forcing or dissipation. Should one throw

Annu. Rev. Fluid Mech. 1986.18:91-147. Downloaded from www.annualreviews.org
by Marine Biological Laboratory - Woods Hole Oceanographic Institution on 04/18/13. For personal use only.

out such problems as unphysical? There are at least three reasons why the answer is no.

Firstly, although physical systems are unable to achieve absolute equilibrium on account of forcing and dissipation, the disparity between equilibrium statistics and physically realized statistics indicates the direction in which nonlinear interactions will *tend* to move a physical system. The physical systems seek to establish the highest entropy states available subject to externally imposed forcing and dissipation.

Secondly, certain quite physically realistic features emerge with absolute equilibrium. Essentially, it is the distribution of variances across wave number that is most affected by dissipation, which is usually presumed to act selectively at high wave number. Cross-correlations such as the degree of barotropy at different scales, the correlation of flow with underlying topography, and even the establishment of basin-scale circulation are not sensitively dependent upon a presence of small-scale dissipation.

Thirdly, how close a physical flow comes to absolute equilibrium may be characterized by a ratio of time scales: an energetic "residence" time compared with a "mixing" or entropy-generation time.

In comparison with equilibrium methods, *disequilibrium* calculations (closure methods) are more tedious and depend upon procedures that are not rigorously established. However, the calculations permit forcing, dissipation, and time-evolving statistics. In comparing closure calculations with the empirical approach based upon numerical simulations, it is noteworthy that closure equations deal directly with statistical quantities and hence do not require averaging across numerical experiments. Relationships among statistical quantities are revealed directly. Dependence of statistical quantities upon external parameters such as β is made explicit so that, for example, derivatives of statistics with respect to β may be evaluated analytically rather than depending upon differencing among sequences of numerical experiments. In many cases, complicated closure expressions permit analytical reduction by systematic approximation procedures.

For the most part, this paper has illustrated the application of equilibrium and disequilibrium statistical mechanics for a variety of geophysical flows. Let us recap just a few points:

1. Maximum-entropy solutions indicate the emergence of predictable, mean, ocean-basin-scale circulation from random initial flow. This result contradicts a popular notion that maximum entropy implies "complete disorder" and hence no large-scale mean flow.
2. A novel account of western intensification is suggested, whereby

Annu. Rev. Fluid Mech. 1986.18:91-147. Downloaded from www.annualreviews.org
by Marine Biological Laboratory - Woods Hole Oceanographic Institution on 04/18/13. For personal use only.

intensification of oceanic currents near western basin boundaries acts as a mechanism for entropy generation. At maximum-entropy equilibrium, western intensification would vanish. The readily observed physical phenomenon is thus viewed as a natural disequilibrium process in ocean circulations.

3. The shape of the main thermocline is seen to emerge spontaneously as a maximum-entropy result.
4. Persistent correlation between geostrophic eddies and underlying topography results from entropy maximization. Disequilibrium calculations extend the maximum-entropy results, producing good agreement with dissipative numerical experiments.
5. Equilibrium arguments provide a basis for anticipating N/f scaling in stratified, geostrophic flow. For bounded flows, the result is to anticipate a tendency toward barotropy on scales larger than the internal deformation radius.
6. Disequilibrium theory provides a unifying treatment ranging from small-amplitude baroclinic instability up through fully developed baroclinic turbulence. Under an imposed meridional temperature gradient, theory predicts both the form and amplitude of a spectrum of poleward eddy heat flux.
7. An extension of equilibrium results for baroclinic flow suggests the enhancement of high-vertical-mode, low-frequency oceanic currents near the equator, as indeed is observed.
8. Disequilibrium study of the transport of passive tracers by geostrophic turbulence obtains the basis for a gradient flux while revealing the role of β-inducing anisotropy among the components of a horizontal eddy diffusivity tensor. Marked differences between transport of vorticity and of passive tracer are identified. An extension to nonconservative tracers provides a simple model for horizontal plankton patchiness in the upper ocean.
9. Entropy provides an information-theoretical measure of the intrinsic degradation of forecast skill with increasing forecast period. Closure theory provides a quantitative account of how geophysical effects such as those due to β may enhance predictability.

Exercises of equilibrium and disequilibrium statistical mechanics provide a wealth of insights, along with detailed quantitative calculations, over a wide range of geophysical fluid phenomena. The reader may foresee further applications. Already we have anticipated that the difficult three-dimensional problem involving interactions among internal inertial-gravity waves and geostrophic modes will be solved. On other points, methodology for disequilibrium calculations admits continuing improve-

Annu. Rev. Fluid Mech. 1986.18:91-147. Downloaded from www.annualreviews.org
by Marine Biological Laboratory - Woods Hole Oceanographic Institution on 04/18/13. For personal use only.

ment. For example, a question concerning the induction of systematic frequency shifts among interacting finite-amplitude waves remains open.

Although the methods discussed in this paper have been illustrated with regard to Eulerian field statistics, corresponding implications for Lagrangian particle statistics have been considered by Kraichnan (1966) and Larcheveque & Lesieur (1981).

In closing it is appropriate to mention two areas in which caution should be observed. The first is the problem of spatial statistical inhomogeneity. Disequilibrium calculations, in particular, are so tedious that they are really only practicable when spatial fields can be expanded upon particularly simple basis functions as $\exp(i\mathbf{k}\cdot\mathbf{x})$. One approach to extending such problems is a quasi-homogeneity expansion, such as that of Carnevale & Martin (1982) or Carnevale & Frederiksen (1983), in which one supposes a two-length-scale separation so that the field fluctuations occur over shorter length scales while the fluctuation statistics vary over a longer length scale. In the limit of infinite scale separation, this kind of inhomogeneity has been included in the baroclinic heat-transport or tracer-stirring illustrations given previously. With limited vertical resolution, Salmon (1980) included vertical inhomogeneity in his studies of two-layer geostrophic turbulence. However, for most cases, if statistics are inhomogeneous on lengths comparable to the energetic eddy scales, then disequilibrium calculations are not yet feasible.

The second point of caution concerns intermittency effects. Both the equilibrium and disequilibrium statistical distributions that have been considered are only up to second order in correlations. If one further supposed distributions to be joint-normal, this description would be complete. At absolute equilibrium such joint-normality is indeed predicted. Numerical experiments for tracer stirring permit a test of this prediction. Holloway & Kristmannsson (1984) have examined various derivative kurtoses, e.g. $K_\nabla(\phi) = \overline{|\nabla\phi|^4}/\overline{|\nabla\phi|^2}$, of tracer fields. For normally distributed ϕ, we have $K = 3$ for all such K. From an experiment without forcing or dissipation, initialized with normally distributed ϕ but with spectra far from equilibrium, Figure 13 shows various $K(\phi)$ rising to supranormal values during the early disequilibrium stage of rapid entropy generation. However, as a maximum-entropy condition is approached, the $K(\phi)$ are seen to relax toward $K = 3$.

Although intermittency vanishes at absolute equilibrium, it is a persistent feature of disequilibrium flows and thus is of concern for realistic applications. Numerical experiments on two-dimensional turbulence (Fornberg 1977, Basdevant et al. 1981, McWilliams 1984) show a characteristic tendency for a vorticity field to "condense" into a collection of relatively isolated vortices. Measuring intermittency by vorticity kurtosis

Annu. Rev. Fluid Mech. 1986.18:91-147. Downloaded from www.annualreviews.org
by Marine Biological Laboratory - Woods Hole Oceanographic Institution on 04/18/13. For personal use only.

K_ζ, McWilliams (1984) reports values of K_ζ up to 40 in some spin-down experiments. Basdevant et al. (1981) suggest that such intermittency effects may account for a steepening in the high-wave-number portions of spectra.

It remains a matter of controversy as to what extent non-joint-normality threatens the exercise of closure theory as in (23). Such theories, which are termed "quasi-normal" are often supposed to depend upon proximity to joint-normality. The fourth cumulant discard in a weak-wave theory, which leads to (20) and (21), is usually argued on a basis of "random-phase approximation" or joint-normality. However, the fact that one calculates an energy transfer because $\langle yyy \rangle \neq 0$ already requires a violation of random phase. Introduction of the coefficient matrix μ leading to (22) further recognizes the violation of random phase. Thus it is in the nature of these closure schemes to suppose nonnormality. The danger is that there is not a deductive basis upon which to determine that departures from joint-normality are being treated approximately correctly. In an effort to assess the skill of closure theory, Herring & McWilliams (1985) make direct comparisons between closure calculations and very high resolution numerical simulations of decaying two-dimensional turbulence. It is found that simulations indeed produce steeper high-wave-number spectra, as also

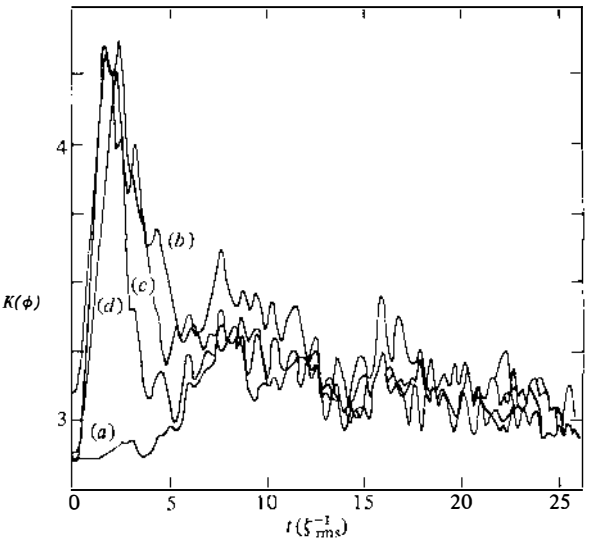

Figure 13 Time evolution of various derivative kurtoses of tracer field ϕ are shown from an unforced, nondissipative numerical experiment. Traces are labeled to show kurtoses of the following quantities: (*a*) ϕ itself, (*b*) $\partial\phi/\partial x$, (*c*) $\partial\phi/\partial y$, and (*d*) $\nabla^2\phi$ (Holloway & Kristmannsson 1984).

Annu. Rev. Fluid Mech. 1986.18:91-147. Downloaded from www.annualreviews.org
by Marine Biological Laboratory - Woods Hole Oceanographic Institution on 04/18/13. For personal use only.

indicated by Basdevant et al. (1981), and that departures of simulation results from closure-theoretical results tend to be larger for larger vorticity kurtoses (near $K_\zeta \approx 9$ in the comparisons by Herring & McWilliams). It may be encouraging with regard to geophysical applications that inclusion of even a very modest value of β has been shown to contain K_ζ at values near 3 (Holloway 1984). Nonetheless, *disequilibrium* flows are seen to exhibit the qualitative impression of intermittency or of "phase-trapping" in coherent structures. Such behavior is not precluded by second-order correlation closure methods but neither is this possible behavior explicitly considered.

Clearly there are limitations, as well as points that are in open doubt, with regard to the statistical mechanics of complicated geofluid systems. However, there are also many applications in which statistical-mechanics methods provide not only insight but also good quantitative skill. The way certainly is open to further application. Resolving some points that are in doubt and overcoming present limitations remain as powerful challenges.

ACKNOWLEDGMENTS

Thoughtful comments were contributed by Ted Shepherd, George Carnevale, Annalisa Griffa, Geoff Vallis, and Jørgen Frederiksen. I am particularly grateful to Rick Salmon for his helpful criticism. Dave Ramsden and Malcolm Smith have provided hitherto unpublished calculations. Billie Mathias typed the draft and Coralie Wallace helped to prepare the figures. Editorial advice and care by the staff at Annual Reviews is sincerely appreciated.

Literature Cited

Allen, K. R., Joseph, R. I. 1985a. Equilibrium statistical mechanics and oceanic internal waves. Preprint (Johns Hopkins Univ./ Appl. Phys. Lab.)

Allen, K. R., Joseph, R. I. 1985b. A canonical Hamiltonian formulation of an oceanic internal wave model including the coriolis effect and geostrophic modes. Preprint (Johns Hopkins Univ./Appl. Phys. Lab.)

Basdevant, C., Sadourny, R. 1975. Ergodic properties of inviscid truncated models of two-dimensional incompressible flows. *J. Fluid Mech.* 69: 673–88

Basdevant, C., Legras, B., Sadourny, R., Beland, M. 1981. A study of barotropic model flows: intermittency, waves and predictability. *J. Atmos. Sci.* 38: 2305–26

Batchelor, G. K. 1969. Computation of the energy spectrum in homogeneous two-dimensional turbulence. *Phys. Fluids* 12: *Suppl. II*, 233–39

Bennett, A. F., Haidvogel, D. B. 1983. Low-resolution numerical simulation of decaying two-dimensional turbulence. *J. Atmos. Sci.* 40: 738–48

Benney, D. J., Newell, A. C. 1969. Random wave closures. *Stud. Appl. Math.* 48: 29–53

Benney, D. J., Saffman, P. G. 1966. Nonlinear interactions of random waves in a dispersive medium. *Proc. R. Soc. London Ser. A* 289: 301–20

Boer, G. J., Shepherd, T. G. 1983. Large-scale two-dimensional turbulence in the atmosphere. *J. Atmos. Sci.* 40: 164–84

Bretherton, F. P., Haidvogel, D. B. 1976. Two-dimensional turbulence above topography. *J. Fluid Mech.* 78: 129–54

Bretherton, F. P., Karweit, M. 1975. Mid-ocean mesoscale modeling. In *Numerical Models of Ocean Circulation*, pp. 237–49. Washington DC: Natl. Acad. Sci.

Carnevale, G. F. 1982. Statistical features of

Annu. Rev. Fluid Mech. 1986.18:91-147. Downloaded from www.annualreviews.org
by Marine Biological Laboratory - Woods Hole Oceanographic Institution on 04/18/13. For personal use only.

Annu. Rev. Fluid Mech. 1986.18:91-147. Downloaded from www.annualreviews.org
by Marine Biological Laboratory - Woods Hole Oceanographic Institution on 04/18/13. For personal use only.

the evolution of two-dimensional turbulence. *J. Fluid Mech.* 122:143–53
Carnevale, G. F., Frederiksen, J. S. 1983. A statistical dynamical theory of strongly nonlinear internal gravity waves. *Geophys. Astrophys. Fluid Dyn.* 23:175–207
Carnevale, G. F., Holloway, G. 1982. Information decay and the predictability of turbulent flows. *J. Fluid Mech.* 116:115–21
Carnevale, G. F., Martin, P. C. 1982. Field theoretical techniques in statistical fluid dynamics: with application to nonlinear wave dynamics. *Geophys. Astrophys. Fluid Dyn.* 20:131–64
Carnevale, G. F., Vallis, G. K. 1984. Applications of entropy to predictability theory. See Holloway & West 1984, pp. 577–92
Carnevale, G. F., Frisch, U., Salmon, R. 1981. *H*-theorems in statistical fluid dynamics. *J. Phys. A* 14:1701–18
Charney, J. G. 1971. Geostrophic turbulence. *J. Atmos. Sci.* 28:1087–95
Edwards, S. F. 1964. The statistical dynamics of homogeneous turbulence. *J. Fluid Mech.* 18:239–73
Errico, R. 1984. The statistical equilibrium solution of a primitive-equation model. *Tellus* 36A:42–51
Fofonoff, N. P. 1954. Steady flow in a frictionless homogeneous ocean. *J. Mar. Res.* 13:254–62
Fornberg, B. 1977. A numerical study of 2-D turbulence. *J. Comput. Phys.* 25:1–31
Fox, D. G., Orszag, S. A. 1973. Inviscid dynamics of two-dimensional turbulence. *Phys. Fluids* 16:169–71
Frederiksen, J. S. 1982. Eastward and westward flows over topography in nonlinear and linear models. *J. Atmos. Sci.* 39:2477–89
Frederiksen, J. S., Bell, R. C. 1983. Statistical dynamics of internal gravity waves–turbulence. *Geophys. Astrophys. Fluid Dyn.* 26:257–301
Frederiksen, J. S., Bell, R. C. 1984. Energy and entropy evolution of interacting internal gravity waves and turbulence. *Geophys. Astrophys. Fluid Dyn.* 28:171–203
Fredcriksen, J. S., Sawford, B. L. 1980. Statistical dynamics of two-dimensional inviscid flow on a sphere. *J. Atmos. Sci.* 37:717–32
Frederiksen, J. S., Sawford, B. L. 1981. Topographic waves in nonlinear and linear spherical barotropic models. *J. Atmos. Sci.* 38:69–86
Garrett, C. J. R., Munk, W. H. 1972. Space-time scales of internal waves. *Geophys. Fluid Dyn.* 3:225–64
Garrett, C., Munk, W. 1979. Internal waves in the ocean. *Ann. Rev. Fluid Mech.* 11:339–69
Green, J. S. A. 1970. Transfer processes of large scale eddies and the general circulation of the atmosphere. *Q. J. R. Meterol. Soc.* 96:157–85
Haidvogel, D. B., Held, I. M. 1980. Homogeneous quasi-geostrophic turbulence driven by a uniform temperature gradient. *J. Atmos. Sci.* 37:2644–60
Haidvogel, B. B., Keffer, T. 1984. Tracer dispersal by mid-ocean mesoscale eddies. Part I. Ensemble statistics. *Dyn. Atmos. Oceans* 8:1–40
Hasselmann, K. 1962. On the nonlinear energy transfer in a gravity spectrum. Part 1. General theory. *J. Fluid Mech.* 12:481–500
Hasselmann, K. 1967. Nonlinear interactions treated by the methods of theoretical physics. *Proc. R. Soc. London Ser. A* 299:77–100
Herring, J. R. 1965. Self-consistent-field approach to turbulence theory. *Phys. Fluids* 8:2219–25
Herring, J. R. 1975. Theory of two-dimensional anisotropic turbulence. *J. Atmos. Sci.* 32:2254–71
Herring, J. R. 1977. Two-dimensional topographic turbulence. *J. Atmos. Sci.* 34:1731–50
Herring, J. R. 1980. Statistical theory of quasigeostrophic turbulence. *J. Atmos. Sci.* 37:969–77
Herring, J. R., McWilliams, J. C. 1985. Comparison of direct numerical simulation of two-dimensional turbulence with two-point closure. Preprint (Natl. Cent. Atmos. Res.)
Herring, J. R., Orszag, S. A., Kraichnan, R. H., Fox, D. G. 1974. Decay of two-dimensional homogeneous turbulence. *J. Fluid Mech.* 66:417–44
Holloway, G. 1975. Thermal equilibration and the statistics of ocean currents. *J. Correct Ocean.* 1:1–19 (Unpublished manuscript)
Holloway, G. 1978. A spectral theory of nonlinear barotropic motion above irregular topography. *J. Phys. Oceanogr.* 8:414–27
Holloway, G. 1979. On the spectral evolution of strongly interacting waves. *Geophys. Astrophys. Fluid Dyn.* 11:271–87
Holloway, G. 1980. Oceanic internal waves are not weak waves. *J. Phys. Oceanogr.* 10:906–14
Holloway, G. 1981. Theoretical approaches to interactions among internal waves, turbulence and finestructure. In *Nonlinear Properties of Internal Waves*, ed. B. J. West, pp. 79–112. New York: Am. Inst. Phys.
Holloway, G. 1982. On interaction time scales of oceanic internal waves. *J. Phys. Oceanogr.* 12:293–96
Holloway, G. 1983a. A conjecture relating

Annu. Rev. Fluid Mech. 1986.18:91-147. Downloaded from www.annualreviews.org by Marine Biological Laboratory - Woods Hole Oceanographic Institution on 04/18/13. For personal use only.

oceanic internal waves and small-scale processes. *Atmos.-Ocean* 21 : 107–22

Holloway, G. 1983b. Effects of planetary wave propagation and finite depth on the predictability of atmospheres. *J. Atmos. Sci.* 40 : 314–27

Holloway, G. 1984. Contrary roles of planetary wave propagation in atmospheric predictability. See Holloway & West 1984, pp. 593–99

Holloway, G., Hendershott, M. C. 1974. The effect of bottom relief on barotropic eddy fields. *MODE Hot Line News No. 65* (Unpublished manuscript)

Holloway, G., Hendershott, M. C. 1977. Stochastic closure for nonlinear Rossby waves. *J. Fluid Mech.* 82 : 747–65

Holloway, G., Kristmannsson, S. S. 1984. Stirring and transport of tracer fields by geostrophic turbulence. *J. Fluid Mech.* 141 : 27–50

Holloway, G., West, B. J., eds. 1984. *Predictability of Fluid Motions.* New York : Am. Inst. Phys. 612 pp.

Hopf, E. 1952. Statistical hydromechanics and functional calculus. *J. Ration. Mech. Anal.* 1 : 87–123

Hoyer, J.-M., Sadourny, R. 1982. Closure modeling of fully developed baroclinic turbulence. *J. Atmos. Sci.* 39 : 707–21

Jaynes, E. T. 1957. Information theory and statistical mechanics. *Phys. Rev.* 106 : 620–30

Kadomtsev, B. B. 1965. *Plasma Turbulence.* London : Academic. 149 pp.

Katz, A. 1967. *Principles of Statistical Mechanics: The Information Theory Approach.* San Francisco : Freeman. 188 pp.

Khinchin, A. I. 1957. *Mathematical Foundations of Information Theory.* New York : Dover. 120 pp.

Kraichnan, R. H. 1959. The structure of isotropic turbulence at very high Reynolds numbers. *J. Fluid Mech.* 5 : 497–543

Kraichnan, R. H. 1966. Dispersion of particle pairs in homogeneous turbulence. *Phys. Fluids* 9 : 1937–43

Kraichnan, R. H. 1967. Inertial ranges in two-dimensional turbulence. *Phys. Fluids* 10 : 1417–23

Kraichnan, R. H. 1971a. An almost-Markovian, Galilean-invariant, turbulence model. *J. Fluid Mech.* 47 : 513–24

Kraichnan, R. H. 1971b. Inertial-range transfer in two- and three-dimensional turbulence. *J. Fluid Mech.* 47 : 525–35

Kraichnan, R. H., Montgomery, D. 1980. Two-dimensional turbulence. *Rep. Prog. Phys.* 43 : 547–619

Kullenberg, G. 1972. Apparent horizonal diffusion in a stratified vertical shear flow. *Tellus* 24 : 17–28

Larcheveque, M., Lesieur, M. 1981. The application of eddy-damped Markovian closures to the problem of dispersion of particle pairs. *J. Méc.* 20 : 113–34

Lee, T. D. 1952. On some statistical properties of hydromechanical and magneto-hydrodynamical fields. *Q. Appl. Math.* 10 : 69–74

Legras, B. 1980. Turbulent phase shift of Rossby waves. *Geophys. Astrophys. Fluid Dyn.* 15 : 253–81

Leith, C. E. 1971. Atmospheric predictability and two-dimensional turbulence. *J. Atmos. Sci.* 28 : 145–161

Leith, C. E. 1984. Minimum enstrophy vortices. *Phys. Fluids* 27 : 1388–95

Leith, C. E., Kraichnan, R. H. 1972. Predictability of turbulent flows. *J. Atmos. Sci.* 29 : 1041–58

Lesieur, M., Herring, J. 1985. Diffusion of a passive scalar in two-dimensional turbulence. Preprint (Natl. Cent. Atmos. Res.)

Lesieur, M., Sommeria, J., Holloway, G. 1981. Zones inertielles du spectre d'un contaminant passif en turbulence bi-dimensionelle. *C. R. Acad. Sci. Paris* 292(2) : 271–74

Leslie, D. C. 1973. *Developments in the Theory of Turbulence.* Oxford : Clarendon. 368 pp.

Levine, R. D., Tribus, M., eds. 1979. *The Maximum Entropy Formalism.* Cambridge, Mass : MIT Press. 498 pp.

Lilly, D. K. 1971. Numerical simulation of developing and decaying two-dimensional turbulence. *J. Fluid Mech.* 45 : 395–415

Lilly, D. K. 1972. Numerical simulation studies of two-dimensional turbulence : I. Models of statistically steady turbulence. *Geophys. Fluid Dyn.* 3 : 289–319

Lin, J.-T., Pao, Y.-H. 1979. Wakes in stratified fluids. *Ann. Rev. Fluid Mech.* 11 : 317–38

Lorenz, E. N. 1969. The predictability of a flow which possesses many scales of motion. *Tellus* 21 : 289–307

Luyten, J. R. Swallow, J. C. 1976. Equatorial undercurrents. *Deep-Sea Res.* 23 : 999–1001

McComas, C. H. 1977. Equilibrium mechanisms within the oceanic internal wave field. *J. Phys. Oceanogr.* 7 : 836–45

McComas, C. H., Bretherton, F. P. 1977. Resonant interaction of oceanic internal waves. *J. Geophys. Res.* 83 : 1397–1412

McComas, C. H., Müller, P. 1981a. Time scales of resonant interactions among oceanic internal waves. *J. Phys. Oceanogr.* 11 : 139–47

McComas, C. H., Müller, P. 1981b. The dynamic balance of internal waves. *J. Phys. Oceanogr.* 11 : 970–86

McWilliams, J. C. 1983. On the relevance of two-dimensional turbulence to geo-

physical fluid motions. *J. Méc. Théor. Appl.* 1983: 83–97 (Suppl.)
McWilliams, J. C. 1984. The emergence of isolated, coherent vortices in turbulent flow. *J. Fluid Mech.* 146: 21–43
McWilliams, J. C., Chow, H. H. S. 1981. Equilibrium geostrophic turbulence. I. A reference solution in a β-plane channel. *J. Phys. Oceanogr.* 11: 921–49
Montgomery, D. 1976. A BBGKY framework for fluid turbulence. *Phys. Fluids* 19: 802–10
Müller, P., Olbers, D. J. 1975. On the dynamics of internal waves in the deep ocean. *J. Geophys. Res.* 80: 3848–60
Müller, P., Olbers, D. J., Willebrand, J. 1978. The IWEX spectrum. *J. Geophys. Res.* 83(C1): 479–500
Müller, P., Holloway, G., Henyey, F., Pomphrey, N. 1985. Nonlinear interactions among internal waves. Preprint (Univ. Hawaii)
Munk, W. H. 1981. Internal waves and small-scale processes. In *Evolution of Physical Oceanography*, ed. B. A. Warren, C. Wunsch, pp. 264–91. Cambridge, Mass: MIT Press
Obukhov, A. M. 1949. Structure of the temperature field in turbulent flows. *Izv. Akad. Nauk SSSR Ser. Geogr. Geofiz.* 13: 58–69
Ogura, Y. 1963. A consequence of the zero-fourth-cumulant approximation in the decay of isotropic turbulence. *J. Fluid Mech.* 16: 33–40
Olbers, D. J. 1976. Non-linear energy transfer and the energy balance of the internal wave field in the deep ocean. *J. Fluid Mech.* 74: 375–99
Olbers, D. J. 1983. Models of the oceanic internal wave field. *Rev. Geophys. Space Phys.* 21: 1567–1606
Onsager, L. 1949. Statistical hydrodynamics. *Nuovo Cimento Suppl.* 6: 279–87
Orszag, S. A. 1970. Analytical theories of turbulence. *J. Fluid Mech.* 41: 363–86
Orszag, S. A. 1977. Statistical theory of turbulence. In *Fluid Dynamics 1973, Les Houches Summer School of Theoretical Physics*, ed. R. Balian, J.-L. Peuve. New York: Gordon & Breach. 677 pp.
Pomphrey, N., Meiss, J. D., Watson, K. M. 1980. Description of nonlinear internal wave interactions by Langevin methods. *J. Geophys. Res.* 85(C2): 1085–94
Pouquet, A., Lesieur, M., Andre, J. C., Basdevant, C. 1975. Evolution of high Reynolds number two-dimensional turbulence. *J. Fluid Mech.* 72: 305–19
Prigogine, I. 1980. *From Being to Becoming.* San Francisco: Freeman. 272 pp.
Rhines, P. B. 1975. Waves and turbulence on a beta-plane. *J. Fluid Mech.* 69: 417–43
Rhines, P. B. 1977. The dynamics of unsteady currents. In *The Sea*, 6: 189–318. New York: Wiley—Interscience
Rhines, P. B. 1979. Geostrophic turbulence. *Ann. Rev. Fluid Mech.* 11: 401–41
Rhines, P. B., Young, W. R. 1982. Homogenization of potential vorticity in planetary gyres. *J. Fluid Mech.* 122: 347–67
Riley, J. J., Metcalfe, R. W., Weissman, M. A. 1981. Direct numerical simulations of homogeneous turbulence in density-stratified fluids. In *Nonlinear Properties of Internal Waves*, ed. B. J. West, pp. 79–112. New York: Am. Inst. Phys.
Rizzoli, P. M. 1982. The stability of planetary solitary waves. In *Topics in Ocean Physics, Proc. Int. Sch. Phys. Enrico Fermi, Varenna, Italy*, pp. 148–83
Rizzoli, P. M. 1984. Coherent structures in planetary flows as systems endowed with enhanced predictability. See Holloway & West 1984, pp. 223–46
Salmon, R. 1978. Two-layer quasi-geostrophic turbulence in a simple special case. *Geophys. Astrophys. Fluid Dyn.* 10: 25–52
Salmon, R. 1980. Baroclinic instability and geostrophic turbulence. *Geophys. Astrophys. Fluid Dyn.* 15: 167–211
Salmon, R. 1982a. The shape of the main thermocline. *J. Phys. Oceanogr.* 12: 1458–79
Salmon, R. 1982b. Geostrophic turbulence. In *Topics in Ocean Physics, Proc. Int. Sch. Phys. Enrico Fermi, Varenna, Italy*, pp. 30–78
Salmon, R. 1982c. Equilibrium statistical mechanics applied to geophysical fluid dynamics. *Proc. GFD Program, Woods Hole Oceanogr. Inst., Rep. WHOI-82-45*, pp. 76–98
Salmon, R., Holloway, G., Hendershott, M. C. 1976. The equilibrium statistical mechanics of simple quasi-geostrophic models. *J. Fluid Mech.* 75: 691–703 (SHH)
Sawford, B. L., Frederiksen, J. S. 1983. Mountain torque and angular momentum in barotropic planetary flows: equilibrium solutions. *Q. J. R. Meterol. Soc.* 109: 309–24
Shannon, C. E., Weaver, W. 1949. *The Mathematical Theory of Communication.* Urbana: U. Ill. Press. 125 pp. 4th printing (1969)
Tang, C., Orszag, S. A. 1978. Two-dimensional turbulence on the surface of a sphere. *J. Fluid Mech.* 87: 305–19
Thompson, P. D. 1957. Uncertainty of initial state as a factor in the predictability of large scale atmospheric flow patterns. *Tellus* 9: 275–95
Thompson, P. D. 1982. On the structure of the hydrodynamical equations for 2-D flow of an incompressible fluid: the role of

Annu. Rev. Fluid Mech. 1986.18:91-147. Downloaded from www.annualreviews.org
by Marine Biological Laboratory - Woods Hole Oceanographic Institution on 04/18/13. For personal use only.

integral invariance. In *Mathematical Methods in Hydrodynamics and Integrability in Dynamical Systems*, ed. M. Tabor, Y. Treve, 88: 301–18. New York: Am. Inst. Phys.

Thompson, P. D. 1983. Equilibrium statistics of two-dimensional viscous flows with arbitrary random forcing. *Phys. Fluids* 26: 3461–70

Tolman, R. C. 1950. *The Principles of Statistical Mechanics*. Oxford: Oxford Univ. Press. 660 pp.

Vallis, G. K. 1983. On the predictability of quasigeostrophic flow: the effects of beta and baroclinicity. *J. Atmos. Sci.* 40: 10–27

Van Kampen, N. G. 1981. *Stochastic Processes in Physics and Chemistry*, Amsterdam: North Holland. 419 pp.

Welander, P. 1973. Lateral friction in the oceans as an effect of potential vorticity mixing. *Geophys. Fluid Dyn.* 5: 173–89

Wiener, N. 1948. *Cybernetics*. Cambridge, Mass: MIT Press. 212 pp.

Williams, G. P. 1978. Planetary circulations: 1. Barotropic representation of Jovian and Terrestial turbulence. *J. Atmos. Sci.* 35: 1399–1426

Young, W. R., Rhines, P. B., Garrett, C. J. R. 1982. Shear-flow dispersion, internal waves and horizontal mixing in the ocean. *J. Phys. Oceanogr.* 12: 515–27

Annu. Rev. Fluid Mech. 1986.18:91-147. Downloaded from www.annualreviews.org
by Marine Biological Laboratory - Woods Hole Oceanographic Institution on 04/18/13. For personal use only.